A STUDY OF MORNING RADIATION FOG FORMATION

THESIS

Jimmie L. Trigg, Captain, USAF

AFIT/GM/ENP/00M-14

DEPARTMENT OF THE AIR FORCE
AIR UNIVERSITY
AIR FORCE INSTITUTE OF TECHNOLOGY

Wright-Patterson Air Force Base, Ohio

Acknowledgments

I would like to take this opportunity to thank the many people who have helped me in this research and preparation of this thesis.

First, I must thank the crew in the weather lab; Pete Rahe, Ed Goetz, Tami Parsons, Liz Boll, Lisa Shoemaker, Mike Holmes and Steve Dickerson. Their help in programming and their understanding during my numerous Tourettes Syndrome like outbreaks made the semester manageable.

Next, I would like to thank my thesis advisor Major Gary Huffines. Our numerous conversations and his suggestions gave me the right amount of assistance to focus and concentrate on the subject when I needed it. He gave me the guidance to step back and see the trees in the forest, and the wisdom not to use a chainsaw to kill a fly.

Last, but certainly not least, I must thank my wife for her friendship and supporting me through my frustrations and helping me with my editing. Without her continuous support I would not have made it through this trial.

Table of Contents

List of Figures

List of Tables

List of Symbols

BR	Visibility obscuration entry indicating fog (Visibility < 1000 meters)
e	Vapor Pressure
e_s	Saturation Vapor Pressure
FG	Visibility obscuration entry indicating fog (Visibility >1000 meters)
HZ	Visibility obscuration entry indicating haze (Visibility <9999 meters)
IDL	Interactive Development Language (computer programming language)
LCL	Lowest Condensation Level
MIFG	Visibility obscuration entry indicating shallow patchy ground fog
NONE	Visibility obscuration entry indicating no obstruction to visibility is Observed
P_{LCL}	Pressure of the LCL
P	Atmospheric pressure
R	Universal Gas Constant (8.3143*10^3 J deg^{-1} $Kmol^{-1}$)
r^2	Coefficient of Determination (1 – (SSE / SST))
SSE	Error Sum of Squares ($SSE = \Sigma(Y\hat{}_i - Y_i)^2$)
SST	Total Sum of Squares ($SST = \Sigma(Y_i - Ybar_i)^2$)
T_{bar}	Average Temperature Between Two Pressure Levels
T	Temperature
T_{LCL}	Temperature of the LCL
Z_{LCL}	Height of the LCL
UTC	Greenwich Mean Time
ρ	Density

Abstract

This research focuses on developing a linear regression formula that forecasters in the Midwest can use to accurately anticipate the formation of radiation fog. This was accomplished in three stages. First a study of the surface and upper air parameters and processes required to develop radiation fog were identified and explored. Next, a linear regression technique was applied to the 23 parameters identified. The top four indicators were then reprocessed and a new linear regression equation was developed. Finally, the new regression equation was compared to an existing fog forecasting technique. The existing forecast technique selected was the 2nd Weather Wings "Fog Stability Index." Hit rates, False Alarm Rates and Threat Scores for both methods were calculated and compared. In general the linear regression, while only accounting for 45 to 50 percent of the total error (SST), outperformed the Fog Stability Index in ability to accurately forecast the development of radiation fog, and greatly reduced the number of incorrect forecasts. The new linear regression equation reduced the false alarm rate on fog forecasting by 23 to 43 percent and increased the threat score ability 30 to 60 percentage points.

A STUDY OF MORNING RADIATION FOG FORMATION

1. Background and Statement of the Problem

1.1. Background

Accurately forecasting radiation fog is a significant problem at many weather stations. "From a meteorological point of view, fog occurrence and severity are hard to predict, and only those forecasters with a good understanding of the local climatology and meteorology are able to demonstrate fog forecasting skill" (Lala 1987). This statement is seen in numerous reviews of missed fog forecasts through the years. The major difficulty in forecasting fog is that similar synoptic conditions that produced fog one morning may not produce fog the next (Lala 1987).

Forecasters usually have all the data they need to forecast the formation of radiation fog accurately, but fail to apply these tools correctly. There has been a great deal of literature written by the Air Force, civilian forecasters, and academic researchers on how fog forms. This literature, unfortunately, has not been effectively crossed to the forecasters.

1.2 Statement of the Problem

Leaders in Weather Stations need a "toolbox" filled with meteorological principles that are grounded in scientific reason and research. Once the governing physical principles of radiation fog formation are fully understood, forecasters can be guided, using the "Funneling Technique," into correctly forecasting the onset and duration of radiation fog. By researching fog formation, centering on tools already accessible to forecasters, and cross feeding this information, weather personnel may be able to improve their overall success rate in forecasting fog that can limit operations.

1.3. Organization

Chapter 2 examines the fundamental processes that contribute to fog formation. In this chapter, each process is defined and explained as to its impact on the development and continuation of radiation fog. In addition, elements readily accessible to the counter forecaster that indicate these processes in motion are noted. Past rules of thumb and simple numerical prediction methods are also listed.

Chapter 3 goes into depth concerning the data required for this research. It covers the data sources, manipulation techniques, computer programs, and filtering schemes employed. The author discusses how missing data was interpolated and how verification data was separated from the main data set.

Results and conclusions are discussed in Chapter 4. Here the regression formula and its verification results are compared to an existing forecasting fog technique.

Finally, Chapter 5 discusses future research opportunities and recommendations for improving the radiation fog formation forecasting skill for Air Force Weather personnel.

2. Radiation Fog Formation Causes and Processes

2.1. Basics Definitions

Ahrens (1988) defines fog as a cloud with its base at the Earth's surface reducing horizontal visibility to less than 1 km. Since fog is defined as a cloud, it stands to reason that it will follow the same "rules" as clouds during formation, dissipation, and advection.

Meteorologists categorize clouds based on their height and structure; so too, fog is divided into four basic types based on its formation process. The four major types of fog are evaporation, upslope, advection, and radiation (Ahrens 1988). The simplest example of evaporation fog is the cloud you see when you exhale outside on a cold day. The warm moisture from your breath saturates the colder air outside causing fog (Ahrens 1988). Upslope fog, as its name implies, forms as air is forced vertically by orographic features. From the ideal gas law, $\mathbf{P=\rho RT}$, air that is forced upward to a lower pressure must cool (Holton 1992). In the equation above, P is the pressure, ρ is the density, T is the temperature of the air parcel and R is the Universal Gas Constant. If this air cools to the dew point, fog forms. In advection fog, the temperature of the parcel decreases or the moisture content increases based on its path and its interaction with the surrounding environment (Ahrens 1988). As air moves into cooler areas, its temperature drops until it is in thermal equilibrium with its surrounding environment. Similarly, an airmass that passes over a moisture source increases its relative humidity until it reaches saturation. Fog forms when this cooling reaches the dew point. Radiation fog forms very similarly to upslope and advection fog; however, radiation fog usually develops, intensifies, and dissipates in a relatively confined area. The air mass cools, not from advection or ascent, but through radiative transfer. This particular type of fog is the most difficult for

forecasters to predict accurately as it initially forms in a very small area and rapidly increases or disappears with apparent randomness.

2.2 Causes

The key processes that produce radiation fog are mixing of different air masses, radiative cooling, rapidly falling pressure, scattering of visible light, adjusting the moisture content of the air mass, and temperature differentials (Fleagle and Businger 1980). The Air Force has reduced this list to two simple processes: increasing the moisture, or decreasing the temperature (AFWA 1998). Forecasters must remember that fog forms not from one particular cause, but from a combination of events (AFWA 1998). "As fog occurs within the boundary layer, a forecaster must focus on the evolution of weather across all scales that may lead to saturation of all or some portion of the boundary layer." (Croft et al. 1997)

a. Mixing

Mixing of adjacent air masses is a major cause of radiation fog. Forecasters must understand the basic principles behind mixing to understand how this process affects fog formation. According to Iribarne and Cho (1980), "If two different adjacent air masses mix, the process occurs essentially at constant pressure," and if there is no condensation, the properties of the resulting mixture will be a mass weighted average of the original parameters. Dew point does not follow this rule. The final dew point for a mixture will be higher than the corresponding linear average of the individual dew points due to the exponential form of the Clausius-Clapeyron equation (Fleagle and Businger 1980). By recalling that the log differential of the specific humidity, and thus the dew point, is equal

to the log differential of the saturation vapor pressure, the Clausius-Clapeyron equation in its empirical, standard atmospheric form reduces to

$$\log10(e_s)=11.40 - 2353/T$$

where e_s is the saturation vapor pressure and T is the temperature of the airmass (Fleagle and Businger 1980). This equation shows vapor pressure of a gas is not a linear function of the temperature of the gas.

According to Iribarne and Cho (1980), a mixture can be represented on a plot of vapor pressure vs. temperature as a point on a line between the initial parameters. However, this can lead to supersaturation of the mixture as illustrated in Figure 2.1. When this occurs, the water vapor in the gas will condense until the mixture reaches the saturation vapor pressure curve.

Forecasters can easily calculate a resulting temperature either from the equation above or by interpolating the graph below. This illustrates that mixing of the atmosphere can result in supersaturation of the lowest levels of the atmosphere, thus contributing to fog formation. It is important to note that although some turbulence is required for the atmosphere to mix and reach saturation or supersaturation values, too much mixing can entrain drier air from aloft into the mixture thus greatly reducing the moisture content. In general, winds speeds less then 2-3 knots will not mix enough of the atmosphere, where winds speeds in excess of 7 knots will entrain dry air (WPAFB LAFP 1999).

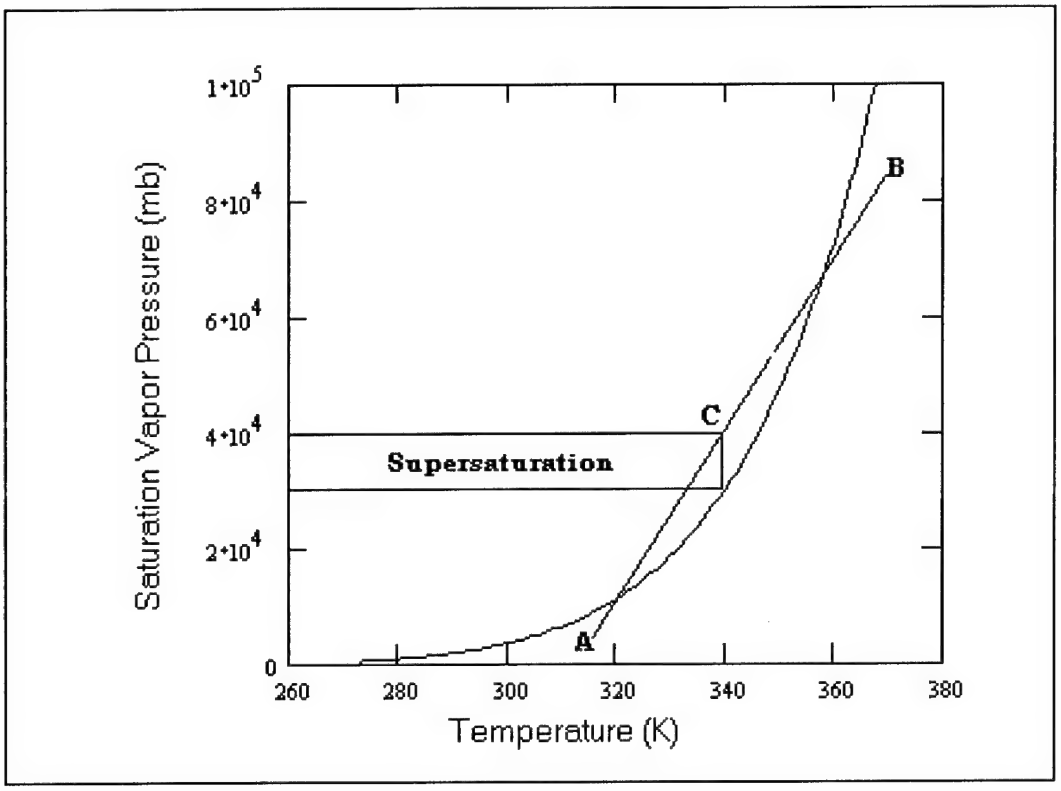

Figure 2.1. Vapor Pressure Vs Temperature. Points A and B indicate the initial conditions. Point C is the mass weighted average temperature and vapor pressure. The air mass at C is supersaturated and must follow the line down to the saturation vapor pressure curve. (Iribarne and Cho 1980)

b. Radiative Cooling

Radiative cooling is another contributing factor to the formation of radiation fog. Radiative cooling is best explained as a system of energy balance equations. Fleagle and Businger (1980) use a parcel of air over a cooling surface to illustrate how the air cools through radiative exchanges. If we assume the air and surface temperature profiles are continuous, the boundary between the air and surface has a given temperature. We also assume that the air in a shallow layer is isothermal. Finally, we also assume that the ground is cooling due to longwave radiation, and that longwave radiation is passing through the airmass without being absorbed. With these assumptions we can create a

system of balancing equations. As the ground cools, energy in the form of heat is transferred from the air just above the ground to the ground. This exchange results in a cooling of the air in the layer just above the ground. As this layer continues to transfer energy to the ground, and thus cool, the air above this layer, which is now relatively warmer, begins to transfer energy into the lower layer, slowing that layers temperature drop. The temperature in the lowest level continues to drop until it reaches either saturation or thermal equilibrium. At this point there may exist a portion of this lower layer where the net exchange in energies going to the ground and coming from the layer above, are balanced and there is no net increase or decrease in temperature (Fleagle and Businger 1980). This forms a temperature inversion where the change in temperature with height equals 0.0.

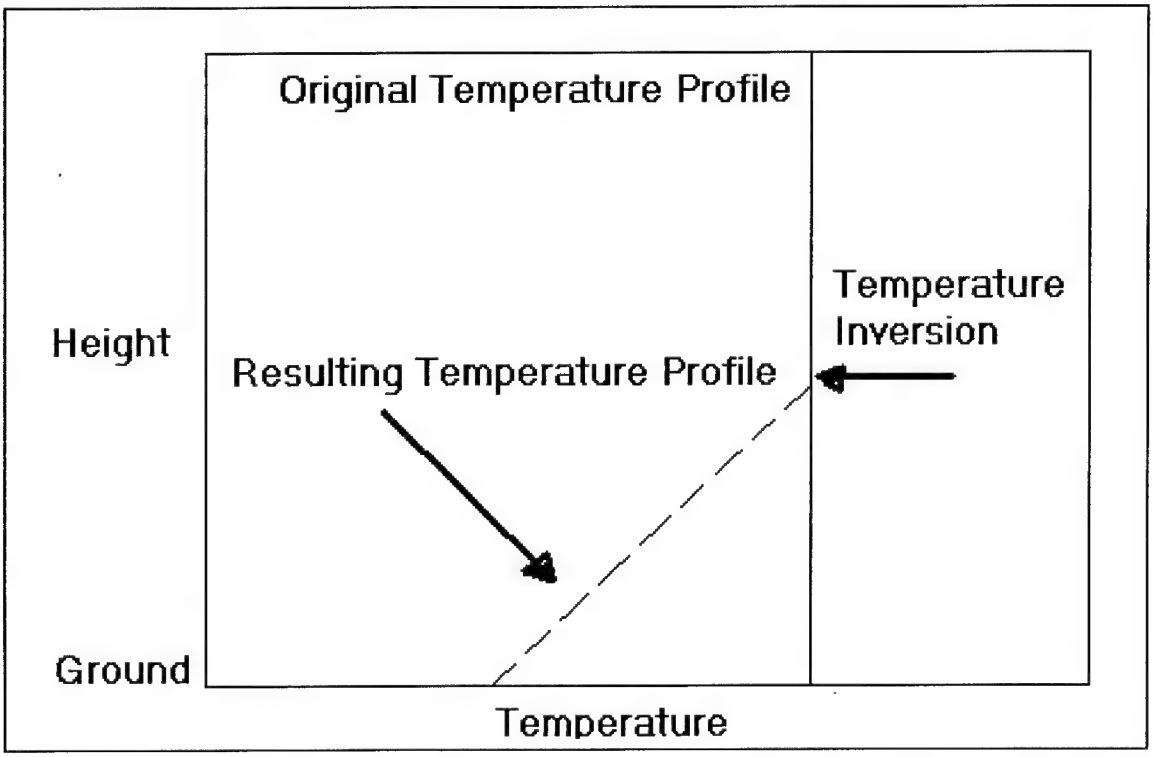

Figure 2.2. Cooling of the Near Surface Airmass. Resulting temperature profile indicates a temperature inversion has formed at the point where the change in temperature with height equals 0.0

Close examination of the evening sounding can give the forecaster a warning that this process is likely to occur. Carefully estimating the amount of warm air advection and taking into account the amount of solar energy imparted to the ground during the day can aid the forecaster in deciding if adequate energy transfer can occur.

c. Rapidly Falling Pressure

An easier and quicker way to create fog is to lower the atmospheric pressure rapidly. Bohren (1987) noted that the air trapped above a carbonated liquid in a bottle is usually twice the sea level pressure of the air outside the bottle. "When the bottle is uncapped, this gas escapes rapidly from the neck and its pressure drops greatly" (Bohren 1987). From the ideal gas law we know that $\mathbf{P=\rho RT}$. When the pressure drops, the temperature and density must change. Since the drop is sudden, the density, and thus the water vapor present in the air, does not have time to decrease. Instead, the temperature drops rapidly to keep pace with the pressure. Consequently, the temperature reaches supersaturation values, and the moisture condenses in the neck of the bottle creating fog.

Although such a drastic event may not appear to be practical in the real atmosphere, rapidly dropping pressures can be a contributing factor to fog formation. The forecaster must recall that fog is not caused by a single event but by a combination of supporting processes. Although pressure drops of a magnitude required to reach saturation are seldom witnessed in the environment, the remark "pressure falling rapidly" in the observation may indicate a sympathetic or supporting process is occurring.

d. Scattering

Scattering is the reason fog is a hindrance to operations. The amount of water vapor in the air does not reduce visibility. Wallace and Hobbs (1977) noted that fog has a

relatively uniform structure over a large horizontal scale, with a liquid water content generally only a few tenths of a gram per cubic meter. Visibility is reduced however, because light interacts with suspended particles. Human eyes are sensitive to a narrow band of radiation in the 0.4 to 0.7 micrometer wavelength known as visible light (Ahrens 1988). Scattering is dependent on the size of the molecule relative to the wavelength of the incident radiation. Fog droplets have an average size of 20.0 micrometer and thus result in near geometric scattering (Schanda 1986). With this scattering, the light from distant objects is refracted in all directions, greatly reducing the amount of light reaching the observer, thus reducing visibility. The initial size of the condensation nuclei plays an important role in how much condensation must accumulate on the particle for it to begin restricting visibility. According to Ahrens (1988), condensation can begin with relative humidities as low as 75%. Therefore, fog can form and restrict visibility even before the temperature reaches the dew point.

In this case, observers play a vital role in forecasting fog formation. A thin haze layer or a slight restriction to visibility in the lowest levels can indicate the presence of condensation nuclei in the atmosphere. Since the visibility is already beginning impaired by the size of these nuclei, it takes a relatively small amount of water vapor condensing on these particles to restrict visibility severely.

e. Moisture

The processes mentioned in the above sections, mixing, radiative cooling, rapidly falling pressure, and scattering all require one common factor to be effective, moisture. Without moisture, there is no condensation at any temperature. Moisture is introduced

into an airmass in several ways; precipitation, evaporation from wet surfaces, and moisture advection are the most common (AFWA 1998).

As rain falls through the atmosphere, it evaporates and thus increases the dew point of the air mass. Once the precipitation has ended, puddles will slowly evaporate adding moisture to the air. Even if there was no precipitation or standing water in the general area, advection can infuse moisture into the airmass.

Advection of moisture can occur by bringing air in from an area that has had precipitation, or by bringing in air that is warmer and has more suspended water vapor. Wind speed and direction are also very important in this respect. Strong winds can cause excessive mixing and inhibit fog formation. On the other hand, air masses that bring additional moisture into the area can be a source of fog.

Plants can also contribute moisture to the atmosphere through transpiration. Griend and Camillio (1986) found that plants, grasses in particular, contributed greatly to the amount of water vapor in the air. They found that grass in excess of 10 cm in length can raise the dew point as much as 1 to 1.5 degrees Celsius during the night. In this case, the forecaster must fully appreciate the events that have occurred to create moisture sources at the station of interest and upstream. In addition, he has to have knowledge of the immediate vicinity of the airfield. Items such as the relative height and condition of the infield grass, succulent crops growing in adjacent fields, and such, are important features to note. Coupled with a sound minimum temperature forecast, the forecaster and observer should note the trend of the dewpoint. Continued evaporation of standing water or advection of moisture will be evident in an increase in the dewpoint. Rapidly falling

temperatures and climbing dewpoint readings should indicate to the forecaster that the potential for fog formation is rapidly increasing.

f. Temperature

Perhaps the most important fog formation parameter after moisture is temperature. The diurnal temperature change is perhaps the single most recognized cause of fog formation. Even the definition of fog formation, "the cooling of air below its dew point", illustrates the importance of temperature (Wallace and Hobbs 1977). Temperature drops can be contributed to two main causes, long wave radiation (Wallace and Hobbs 1977) and evaporation (AFWA 1998).

During the night, solar radiation is cut off, and the earth begins to cool. Long wave radiation is released from the earth skyward (Iribarne and Cho 1980). If there are no clouds to absorb or reflect this radiation then the surface will cool rapidly. Once the surface cools, the actions cited in the irradiance section become the dominant process. The air cools until it reaches thermal equilibrium. This equilibrium point could be saturation, in which case fog forms, or radiative transfer equilibrium where the exchange of heat with the air and ground balance at a temperature above saturation values.

When calculating the temperature equilibrium point, forecasters often dismiss evaporation. Condensation is the mechanism for drawing moisture from the air and forming fog; however, evaporation can occur during the day adding moisture and through the early part of the night cooling the air to the saturation point. Once the air cools, added moisture through transpiration, continued evaporation of standing water, or moisture advection can produce fog. Once dew forms, it is a common belief that fog will not form. Forecasters must be wary of applying this rule blindly. Dew can be a ready

source of moisture under the right conditions. In the same way, nearby golf courses that water during the night may be setting the stage for a major fog incident.

Diurnal temperature curves, developed by the Air Force Combat Climotology Center in Asheville, North Carolina and delivered to every Base Weather Station in tabular format, can assist forecasters in determining the amount of cooling to expect during the night. These tables are specifically developed for each station and are stratified into month, cloud cover, wind speed and wind direction. These tables give the forecaster a good "first guess" of the expected minimum temperature (AFWA 1998).

Another method for forecasting the minimum temperature is to employ the equation below. This equation was developed by J. M. Craddock and D. Pritchard to assist in forecasting fog; the temperatures are in degrees Fahrenheit (AFWA 1998).

Tmin = 0.32*(Temperature at noon) + 0.55*(Dew Point at noon) + 2.12 +C

Table 2.1. Variable used in Craddock and Pritchard Equation. C is a variable dependent on the wind speed and mean cloud amount.

Mean Forecast Surface Winds	Cloud Amount 0-1/8	Cloud Amount 2/8 – 3/8	Cloud Amount 4/8 – 5/8	Cloud Amount 6/8 – 8/8
< 10 Kt	-3	-2	-1	0
> 10 Kt	-1	0	0	+1

A critical factor when forecasting the minimum temperature is that condensation itself can release heat into the environment. The cooling mechanism must not only be strong enough to cool the air to the saturation point but overcome the latent heat of condensation released. As water vapor condenses on a nucleus, it releases heat. Although for this process the parcel is not lifted, the temperature change and heat release can be modeled using the equation listed below (Wallace and Hobbs 1977).

- L*dws=Cp*dT + G*dz

Here L is the latent heat of condensation, dws is the saturation mixing ratio. Cp is the specific heat at constant pressure for dry air. dT is the change in temperature of the parcel. And G*dz is the force acting on a parcel as it is lifted. This equation illustrates how as the parcel cools (dT<0) at a constant height (g*dz=0) the energy released by condensation, in the form of heat (L*dws), is greater then zero. So as condensation begins due to cooling, heat is released to counter the cooling. In certain circumstances, this latent heat release may equal the effects of radiational cooling, keeping the temperature constant. This is a very important principle that must remain foremost in the forecaster's mind during marginal fog events.

2.3 The Five Stages of Fog Formation

Garland Lala, in his paper "Radiation Fog: Characteristics and Formation Processes" (1987) divides the fog formation process into five distinct phases. These five phases outline the processes that occur through the night that result in operations-inhibiting fog at sunrise. By understanding these different stages and how each fog forming process works within them, forecasters can better anticipate the timing and intensity of operations-inhibiting fog.

The first phase starts at sundown. A rapid temperature drop due to radiational cooling of the atmosphere characterizes this phase. According to Lala (1987), this cooling rate can be as much as 2 to 3 degrees Celsius per hour. During this phase, the near adiabatic lapse rate during the day is replaced with a strengthening temperature inversion, which will act to isolate the low level air and moisture from the drier air aloft. It also reduces the surface winds and the possibility of mixing. This cooling with little mixing acts to increase the relative humidity of the surface air (Lala 1987). During this phase, observers

may notice a slow but steady decrease in horizontal visibility as condensation forms on suspended hydroscopic particles.

The second phase begins two to three hours after sundown and lasts for the next eight hours (Lala 1987). The temperature cooling rate drops to one degree Celsius per hour and works to strengthen the inversion. Here the inversion may grow to 100 to 150 meters from the ground while the air under the inversion is nearly saturated (Lala 1987). Short-lived patches of fog form and move through the area. These patches could be missed at a station with a limited meteorological watch. Close scrutiny of the Runway Visual Range detector could be the only indicator that fog is imminent.

After about 0500 local time the mature fog stage begins (Lala 1987). The air is saturated at the lower levels, and the maximum radiational cooling moves to the top of the fog layer (Lala 1987). Fog begins to thicken and increase in depth as the air above cools rapidly.

Most forecasters are familiar with the term "sunrise surprise." As the sun rises, the top of the inversion is heated and turbulent fluxes develop. In most cases this would act to inhibit fog formation (Lala 1987). However, in this instance it acts to intensify the fog by thoroughly mixing the saturated air and providing even more moisture through surface evaporation. This is the major characteristic of the fourth phase in fog development. This phase is easily identified by the transition from a smooth surface above the fog to an irregular boiling like texture as the fog mixes (Lala 1987).

Finally, the increased solar radiation begins to heat the surface to an extent that the associated convective circulations mix the saturated air with the drier air aloft breaking the inversion and dissipating the fog (Lala 1987). This phase can happen rapidly based

on the amount of incoming radiation and mixing. Direct absorption of solar radiation by the atmosphere can play a role in fog dissipation, but the increased mixing due to convection often overwhelms its effects (Lala 1987).

2.4 Fog Forecasting Techniques

A quick review of any weather station's forecast review binder will list nearly as many ways to forecast fog as there are forecasters. Some "rules of thumb" work well, and some are happenstance. Those based, even if unknowingly, on the physical principles of fog formation are the most reliable. To anticipate radiation fog accurately, the forecaster must understand the stability of the atmosphere, calculate the minimum temperature for the night and the corresponding dew point, factor in the wind speed and direction, and be familiar with moisture sources in the area and upstream.

a. Rules of Thumb

Fog formation is a fine line between mixing and stratification of two air masses. One of TSgt Ritchie's, Senior Forecaster at Wright-Patterson AFB (Ritchie 1996), favorite "rules of thumb" was that fog is unlikely if the lights of the near by city are "twinkling". At first, this may seem insignificant, but this rule does have scientific merit. The "twinkling" of the lights indicates the index of refraction for the air is changing. Much like a shimmering mirage in the desert, it's indicative of vertical motion, which will mix the low level moisture with drier air aloft inhibiting fog formation.

b. Simple Numerical Predictors

Very similarly, Herr Strauss, from the 2nd Weather Wing, USAF developed the "Fog Stability Index" based on the difference between the 850 mb and surface parameters (AWS 1990).

$$FI = 4*T_s-2*(T_{850}+T_{ds})+W_{850}$$

FI>55	**Fog threat is low**
32< FI<55	**Fog threat is moderate**
FI <31	**Fog threat is high**

Here T_s is the temperature at the surface in degrees Celsius. T_{850} is the temperature at 850 mb in degrees Celsius. T_{ds} is the surface dew point temperature in degrees Celsius. And W_{850} is the 850 mb wind speed in knots.

This formula illustrates how important the upper level winds and temperatures are in forecasting fog. If the 850 mb winds are too high, turbulent eddies will mix the layer, likewise, if the 850 mb temperature is too low, the atmosphere will be unstable, and convective eddies will mix the upper and lower air. Recall that fog needs a stable but very lightly mixed atmosphere for development.

This formula and its verification are discussed in Chapter 4. At this point, it is important that the forecaster understand that this formula gives only an index. It does not indicate the intensity or duration of the fog event, only that fog is possible given the parameters in this formula.

3. Data Analysis

3.1 Selection of Data Sets

The 88th Weather Squadron at Wright-Patterson Air Force Base, Ohio, sponsored this thesis. The weather squadron requested assistance in forecasting the formation of early morning radiation fog. On average, the base weather station experiences 187 days of fog per year (AFCCC 1999). The location and general topography around the base favors the formation of radiation fog.

The base weather station is located in the wide Miami River Valley approximately eight miles from the center of Dayton, Ohio (WPAFB TFRN 1999). This proximity to the city provides a source of condensation nuclei on days with a strong inversion.

The surrounding area is also rich in ready sources of moisture. The Mad River flows along the western edge of the airfield. There are also14 small ponds and lakes in and around the airfield. In addition, the Huffman Dam lies just south of the runway complex. This makes the south end of the overrun susceptible to local flooding (WPAFB TFRN 1999).

Topography also assists in the formation of fog by mixing of atmosphere. The higher elevations to the northeast develop a drainage wind during nights with a strong inversion. This could provide the light, cool breeze required for the mixing and formation of radiation fog (WPAFB TFRN 1999).

In order to expand the utility of this thesis, two additional Air Force Base Weather Stations were selected. By selecting these additional stations, more data points are introduced into the regression, which mitigates local effects, and develops a forecasting

tool concentrating on the most significant causes of radiation fog instead of the local indicators.

The two additional sites selected were Scott Air Force Base, Illinois, and Ft Campbell Army AirField, Kentucky. Both stations are in the "Midwest", have a significant number of days with fog, and have a basic meteorological watch, meaning their observing functions do not close at night.

Scott Air Force Base has on average 197 days with fog (AFCCC 1999). Like Wright-Patterson, Scott's location and topography play a major role in fog formation. Scott lies in the Silver Creek Valley 16 miles southeast of downtown St. Louis, Missouri (Scott TFRN 1999). In addition to the proximity of the major city, Scott is surrounded by farm lands which add greatly to the condensation nuclei especially during the early spring and late fall seasons due to increased agricultural activities.

Similar to Wright-Patterson, Scott has two major land features which enhance mixing of the lower boundary layer during strong inversions. Shiloh Hill, is two miles to the northwest and Turkey Hill is five miles to the southwest. Both hills rise 200 to 300 feet above the airfield elevation and provide drainage winds to mix the layer.

Moisture sources are also evident in and around Scott's airfield. Silver Creek runs north to south along Scott's runway and forms a swamp one to two miles southeast of the complex. This swamp can act as a moisture source after heavy rains and a light southeasterly wind.

Ft Campbell Army Airfield has on average 170 days with fog (AFCCC 1999). It also has significant proximity and orographic influences which enhance the formation of radiation fog. Ft Campbell is located in a shallow east-west valley, which lies along the

Kentucky-Tennessee State line. Terrain rises of 200 feet approximately 20 miles to the north and south of the airfield act as sources for drainage winds. Moisture sources include the Kentucky Lake and Lake Barkley located 25 miles west of the complex (Ft Campbell TFRN 1999).

Data sets were restricted to the years 1990 to 1997. This ensured observation points and equipment were reasonably standardized and that the data was as close to uniformly formatted as possible. Items to take into consideration were that in 1992, the Air Force implemented the Automated Weather Dissemination System (AWDS), and in 1994-1995 the AWDS system had a software upgrade, which affected the formatting of the surface observations. Then, in 1996, the Air Force transitioned from using Surface Airways code to the international METAR code. In addition, in 1995, the National Weather Service underwent regionalization, relocating several upper-air stations to new Regional National Weather Service Station locations.

3.2 Data Sets and Format

Data sets included surface observations from the three selected sites along with the upper air soundings from the nearest sounding station. For Wright-Patterson, this was the Dayton National Weather Service office from 1990 to 1995, and the Wilmington Regional National Weather Service office from 1995 to current. For Scott, the nearest upper-air station was the Peoria National Weather Service office from 1990 to 1995, which then transferred to the Lincoln Regional National Weather Service office from 1995 to present. The author did not adjust for distance or bearing from the sounding station to the forecast location in question, since these stations are the closest upper-air data site for each base weather station, and thus the soundings were assumed to be

representative for synoptic-scale weather. Ft Campbell was the only station not to have an upper-air sounding station shift. For Ft Campbell the upper-air station was Nashville National Weather Service office from 1990 to present.

The Air Force Combat Climatology Center (AFCCC), in Asheville, North Carolina, provided all the data for this research. This center is the repository for all weather data from military and civilian reporting stations throughout the world. They were able to provide the surface observations in a "Microsoft Excel" spreadsheet format. In addition, the upper-air data was provided in a delimited text format for import into a spreadsheet or computer program.

Although the author requested the data in such a way as to reduce formatting anomalies, several data formatting changes had to be accomplished before all the data could be compiled. First, some of the data sets had the date group reported in year, month, day format (YYMMDD). The author separated this entry into its components for data filtering. Similarly, the wind data varied slightly over the years. Some data sets had the wind reported in direction, speed and gust (DDDSSGG). This was de-coupled into its base parts. In addition, simple reformatting was accomplished in order to ingest the data into the equations used to develop the parameters used in the regression. For example, the ceiling remarks in the observations begin as "cig", "cigm", "cige" or "vv" to indicate a basic ceiling remark, a measured ceiling remark, an estimated ceiling remark or a vertical visibility remark respectively. The author removed these prefixes, thus creating a numerical indicator. Pressure alos had to be standardized. Some pressure entries were in four digits without a decimal point (3002), whereas most had the decimal point reported (30.02) (inches of Hg). All pressure readings were formatted to have the decimal point.

3.3 Interpolating Missing Data and Combining Surface/Upper-Air Observations

Some data entries required a more in-depth analysis. For example, missing visibility readings, obscurations, and ceiling remarks had to be manually interpolated and filled in. For the most part these missing data points centered on the introduction and subsequent upgrades to the AWDS system. In these cases, the base weather stations were notified that there were potential problems with the encoding subroutines so plain text observations were recorded in the remarks section of each observation during these times. Recovering this data required the author to sort through 24 years of data (three stations, eight years for each station) and fill in the missing blanks from the remarks section, if available. In some cases, the missing data was not available in the remarks section. In these cases, the author relied upon his nine years as a certified weather forecaster and the remaining parts of the observation to estimate the values. When in doubt, the author deleted the entire observation, rather than contaminate the data set.

The author assumed some parameters were linearly dependent over short time spans or distances when interpolated. These included the surface pressure, temperature, dew point and upper level temperature and dew point. It was assumed that the pressure and temperatures did not wildly fluctuate over the course of one hour or that the temperatures did not "spike" positively or negatively within 1,000 feet vertically. For these interpolations, computer programs written in "Interactive Data Language" (IDL) were used. One program was used to interpolate surface data and one specifically for the upper-air data. (See Appendix A.1 and A.2 respectively.)

IDL programs were also used to reduce the upper-air data sets (see Appendix A.3). The typical sounding extends from the surface to approximately 100 millibars

(53,000 feet above ground level (AGL)). Since fog is limited to the lowest levels of the atmosphere, the upper-air data sets were truncated at 700 millibars (10,000 feet AGL). This ensured the data set had upper level values to interpolate any missing 850 millibar (5,000 feet AGL) values. The 850 millibar level was required for verification of the Fog Stability Index referred to in Chapter 2.

After the upper-air data was truncated, it was sent through another IDL program with the corresponding surface data (see Appendix A.4). This program compared the date and time of the surface data point and appended the matching upper-air data to the end of the observation. For example, surface data from 1 January, 1990, 0000 UTC to 1159 UTC had the upper-air 1 January, 1990, 0000 UTC 850 millibar temperature, dew point, wind direction and wind speed appended. This combined both data sets into one file clearly illustrating the surface and upper-air parameters at the time of the observation.

3.4 Development of Radiation Fog Indicators

Now that the surface and upper-air data sets are compiled in such a way that each observation is a "snap-shot" of the conditions at the surface and at 5,000 feet, proposed indicators can be derived that vary with each observation.

Recall from Chapter 2 that the most probable causes of radiation fog are moisture, pressure falls, radiational cooling, condensation nuclei, mixing, and a shallow boundary layer. With these parameters in mind, indicators were derived from the combined observations.

To indicate a ready moisture source, a column was created to indicate if precipitation was occurring in that observation. A zero was entered if the obscuration entry was, "NONE", "BR", "FG", "HZ" or "MIFG", and a one was entered for any other

weather phenomenon. Then a column was created that summed the values in the precipitation indicator column in groups of 12. This column gives an estimation of the number of hours precipitation was occurring over the last 12 hours (0-12).

Another moisture indicator was relative humidity. Relative humidity (RH) is the ratio of vapor pressure (e) to the saturated vapor pressure (e_s). To calculate relative humidity the vapor pressure and saturated vapor pressure had to be calculated using the formulas listed below (Rogers and Yau 1989).

e=6.112*EXP((17.67*Dew Point)/(Dew Point+243.5))

e_s=6.112*EXP((17.67*Temperature)/(Temperature+243.5))

RH=e/e_s

With these formulas, the relative humidity was calculated for each observation. However, according to Ahrens (1988), condensation can begin with relative humidities as low as 75%. Thus, fog can form and restrict visibility even before the temperature reaches the dew point. Therefore, it may prove important to look at the rate of change of temperature, dew point and relative humidity over 12 hours.

To get an accurate rate of change over time, all "special" observations were removed. "Special" observations are observations taken between hourly observations and indicate conditions that have transitioned through specified criteria such as ceiling height or beginning and ending of precipitation. These "specials" were taken into account during the manual and automated interpolation phases but are now of limited use. With the removal of the "specials" every 12 observations directly implies 12 hours of time has transpired.

The temperature and dew points were converted from degrees Celsius to Kelvin to remove the negative signs. Then the current temperature or dew point was subtracted from the 12-hour previous reading to get a rate of change over 12 hours. Similarly, the current relative humidity was subtracted from the one 12-hour previous to get the rate of change of the relative humidity over 12 hours.

As the surface pressure is included in each observation, it was easy to calculate a pressure change over 12 hours. Like the temperature above, the current pressure was subtracted from the previous 12-hour pressure reading resulting in a rate of change of pressure over 12 hours.

Radiational cooling was parameterized using the ceiling entry. Each observation has a ceiling remark that ranges from 000 (totally obscured with no separation between the ground and the vertical obscuration) and 300 (at least 5/8ths of the sky is cumulatively obscured up to 30,000 feet). In addition, the author added the value 310 to indicate that there was less then 5/8ths of the sky covered, or no ceiling present. A column was created and assigned a value of zero if the ceiling entry was less then 250, a ceiling was present below 25,000 feet. A value of one was entered if the value was greater then 250, i.e., no ceiling was present below 25,000 feet. Then, like the precipitation indicator, the data was summed over 12 hours to give a cumulative number of hours with a ceiling above 25,000 feet (0-12). In addition, an indicator was developed that recorded the ceiling height 12 hours before the current observation. This would indicate the amount of radiation being added to the earth during the day or radiated out during the night.

Next, the condensation nuclei parameter was developed. With this, the author looked at the visibility obscuration to see if "HZ" (haze) was reported. Recall again that in Chapter 2 the size of the condensation nuclei is important to the severity of the fog event. It is assumed that if haze was reported in the observation, there are particulates suspended in the air that are already reducing visibility. A column was created with a value of one if the obscuration was "HZ" and a zero if any other value. Then these values were summed over 12 hours (0-12).

These methods left 12 observations a year without corresponding readings. Thus, the first 12 observations in each year were deleted (252 observations). Since the total number of observations used in this thesis was in excess of 170,000 these deleted observations were approximately one tenth of one percent and thus deemed statistically insignificant.

The next parameter investigated was mixing. Excessive wind speed could entrain dry air into the boundary layer thus inhibiting fog formation. Based on the Wright-Patterson fog decision checklists (WPAFB LAFP 1999), five knots was selected as the cut-off value between mixing and dry air entrainment. Thus, any observation with wind speeds above 5 knots was deleted.

Finally, the boundary layer was parameterized using three formulas listed below from the Air Weather Service Technical Report 83-001 (Duffield and Nastrom 1983). These formulas calculate the temperature of the Lowest Condensation Level (LCL), pressure of the LCL, and height of the LCL, based on a standard dry adiabatic lapse rate.

$$\textbf{Temperature}_{LCL} = (T_d)-(0.212+(0.001571*(T_d))-(0.000436*(T)))*(T-T_d)+273.16$$

$$\textbf{Pressure}_{LCL} = P*((T_{LCL}/(T+273.16))^{(1/0.2854)})$$

$$\textbf{Height}_{LCL} = (((287*(((T+273.16)-(T_{LCL}))/2))/9.8)*LN(P/P_{LCL}))$$

Here T_d (dew point), T (temperature) and P (pressure) are all measured at the surface. T_{LCL} is a derived value using the first equation and P_{LCL} is a derived value from the second equation. Surface temperatures and dew points are reported in degrees Celsius. T_{LCL} is in degrees Kelvin. Pressure values are reported in inches of mercury and the height is reported in meters.

All these transformations resulted in an "Microsoft Excel" spreadsheet with 41 columns and over 170,000 lines representing the conditions for the three locations for each hour from 1 January 1990 to 31 December 1997. Of those 41 columns, 23 were imported into the regression calculations and are listed in Table 3.1. These parameters are broken into four subcategories. First, the values the forecaster can not readily update such as the upper-air values are listed. Next is the rate of change parameters such as the pressure change over 12 hours. The third set of parameters were ones the forecaster routinely forecast, such as the forecasted wind speed and direction. The final parameters were ones that had to be calculated such as the temperature of the LCL.

Table 3.1. List of Parameters. These parameters were investigated to determine their significance in radiation fog formation.

Fixed Values	**Forecasted Values**
Month	Wind Direction
850mb Temperature	Wind Speed
850mb Dew Point	Surface Temperature
850mb Wind Speed	Surface Dew Point
850mb Wind Direction	Surface Pressure
Ceiling 12 hours ago	Ceiling
	Relative Humidity
Rate of Change Values	**Calculated Values**
Change in Pressure over 12 hours	Temperature of the LCL
Change in Temperature over 12 hours	Pressure of the LCL
Change in Dew Point over 12 hour	Height of the LCL
Change in Relative Humidity over 12 hours	# Hours Ceiling >25,000' in 12 hours
	# Hours of Precipitation in 12 hours
	# Hours of Haze in 12 hours

At this point the 1997 data from each site was extracted and set aside to act as the verification data set. This set, one from each location, represents 12 percent of the total data used. Since the weather events that occur in January of 1996 have no impact on the weather events for January 1997, it is assumed that this portion represents a random sample of the data.

4. Analysis and Verification

4.1 Verification of Assumptions

a. Timing of Radiation Fog Events

The first assumption made in this thesis is that most radiation fog events occur in the early morning hours. This assumption was based on the writing of Lala discussed in Chapter 2 and the author's experiences as a counter forecaster. In order to verify the assumption a single year's worth of data was selected from each forecast site. All observations containing fog (BR, FG, MIFG) in the visibility obscuration column were selected. This reduced data set was then plotted verses time in a histogram, Figures 4.1 through 4.3. As can be seen, the histograms appear to be normally distributed about a central mean of between 1100 and 1200 hours UTC.

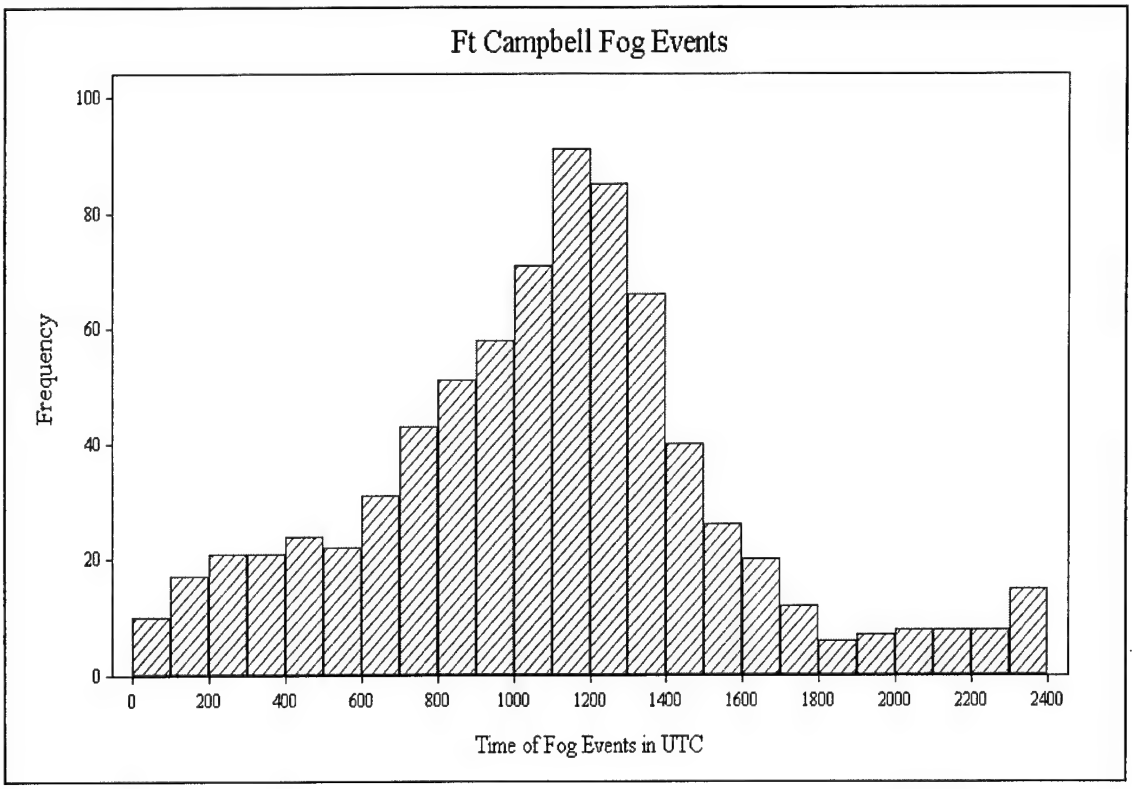

Figure 4.1. Ft Campbell Fog Timing Histogram. Time of Observation (UTC) carrying fog versus the frequency of that event.

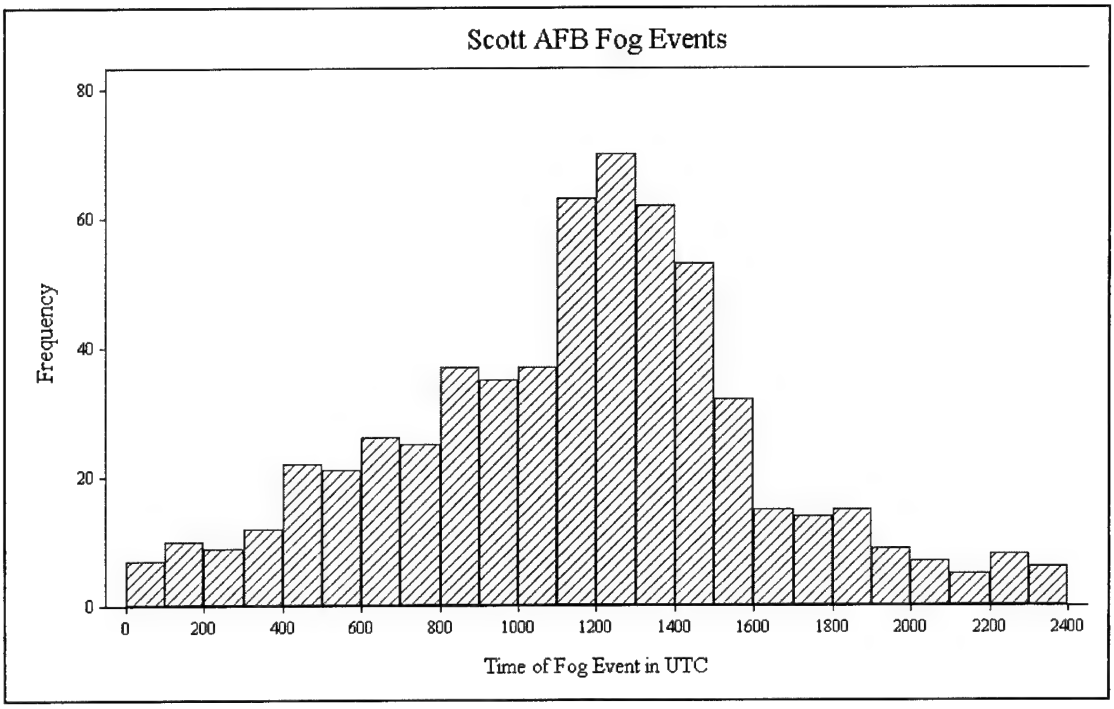

Figure 4.2. Scott AFB Fog Timing Histogram. Time of Observation (UTC) carrying fog versus the frequency of that event.

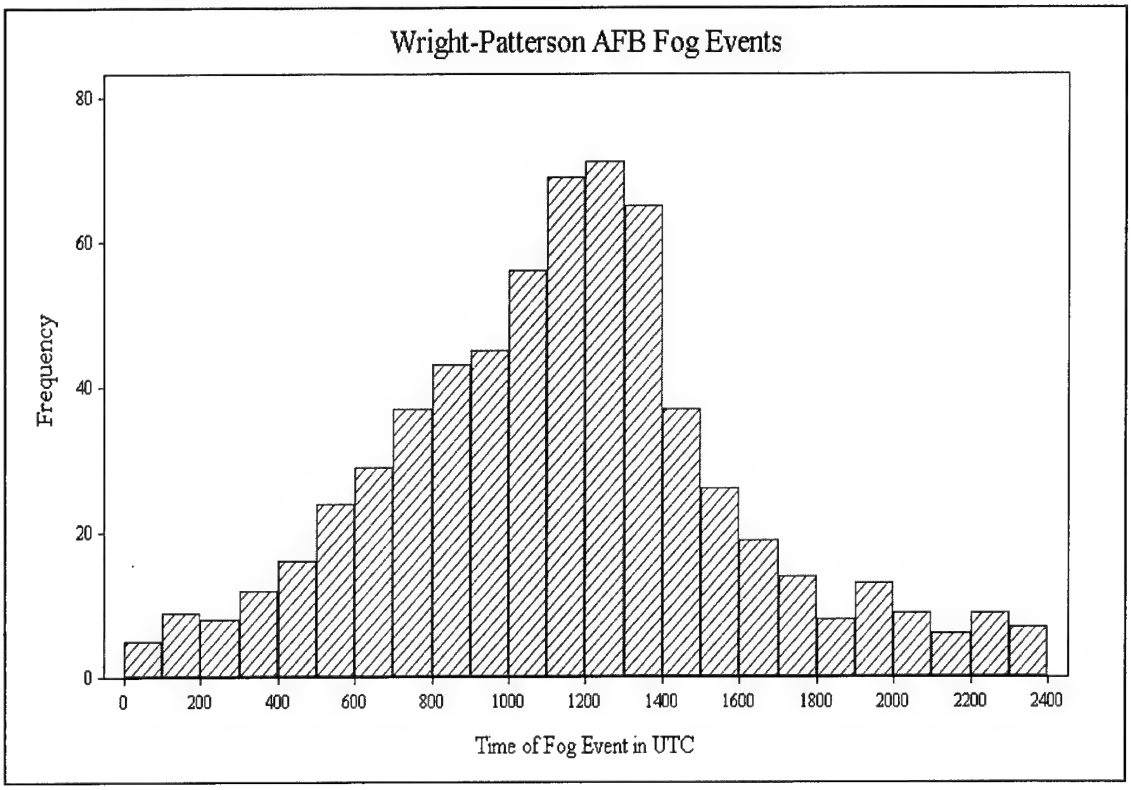

Figure 4.3. Wright-Patterson AFB Fog Timing Histogram. Time of Observation (UTC) carrying fog versus the frequency of that event.

b. Normality of the Data

In order to verify that the distributions are approximately normally distributed a Wilk-Shapiro/Rankit test was performed on the data using the computer program "Statistix". The Wilk-Shapiro/Rankit Plot procedure examines whether a variable conforms to a normal distribution. The *i*-th rankit is defined as the expected value of the *i*-th order statistic for the sample, assuming the sample was from a normal distribution. The order statistics of a sample are the sample values reordered by their rank. If the sample conforms to a normal distribution, a plot of the rankits against the order statistics should result in a straight line, except for random variation. The approximate Wilk-Shapiro statistic calculated is the square of the linear correlation between the rankits and the order statistics (0-1). Systematic departure of the rankit plot from a linear trend indicates non-normality, as does a small value for the Wilk-Shapiro statistic. One or a few points departing from the linear trend near the extremes of the plot are indicative of outliers. In this case, the resulting Wilk-Shapiro statistics were 0.9847 for Wright-Patterson, 0.9854 for Scott, and 0.9749 for Ft Campbell. This illustrates that the distributions are approximately normally distributed. Figure 4.4 shows the Wilk-Shapiro results for Wright-Patterson AFB. The other bases results were similar.

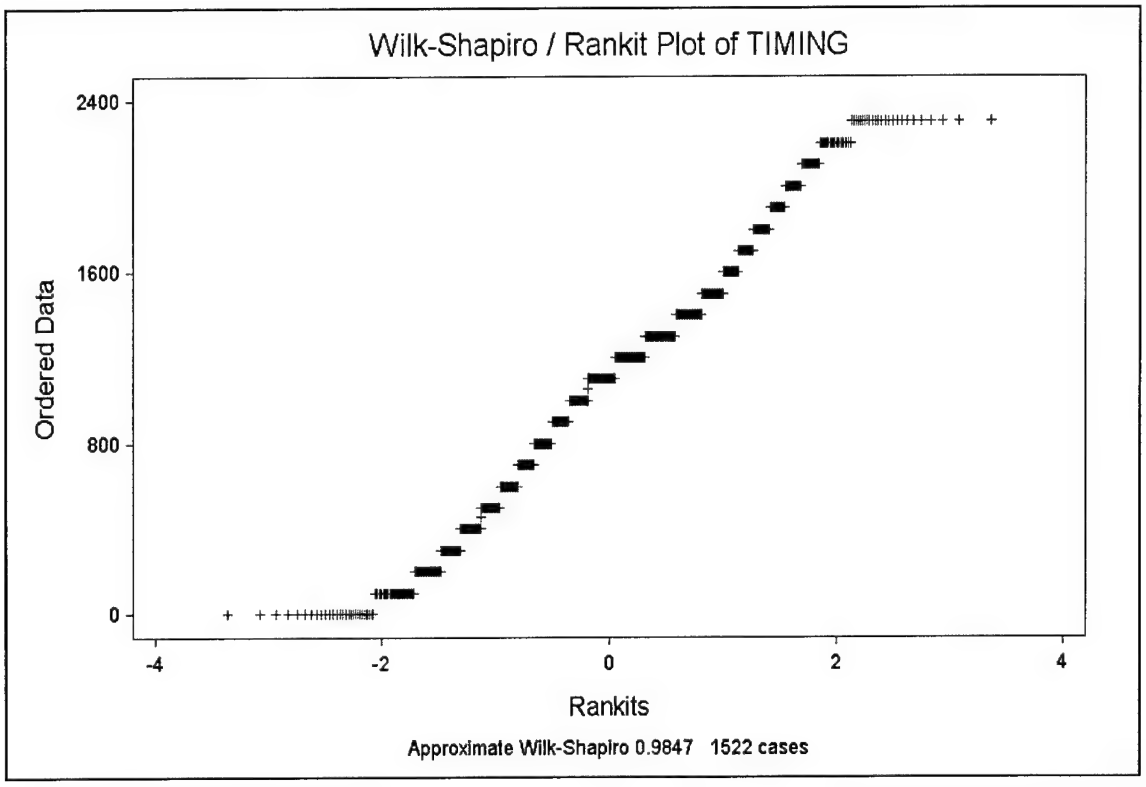

Figure 4.4. Wilk-Shapiro Resultant Plot. This test for normality for the data from Wright-Patterson AFB. A score of 0.9847 indicates that the data can be assumed normally distributed.

4.2 Principles of Statistics Used

After establishing normality, it is assumed that each ordered pair, predictor and resultant can be described by the linear equation,

$$Y_i = \beta_0 + (\beta_1 * X_i) + \varepsilon_I \qquad \text{(Devore 1995).}$$

In this equation, the resultant, Y_i, is assigned the value of the visibility for the point in question. Likewise, X_i is assigned the value of the predictor or parameter of interest, e.g., relative humidity and ε_i is the residual error associated with using an estimated linear regression versus the true regression. It can be visualized as the distance from the data point to the estimated line along a constant X. The subscript i indicates each of the

ordered pairs used in the regression. The intercept and slope of the line are defined by β_0 and β_1 respectively, which are calculated by minimizing the residual error.

The residual error is calculated by squaring the difference between the estimated regression line and the true regression line

$$f(\beta_0,\beta_1) = \Sigma (y_i - Y_i)^2 = \Sigma (y_i - (\beta_0 + (\beta_1 * X_i)))^2$$

where y_i is the value of the dependent variable for the true regression line (Devore 1995). For this example, the best fit regression line is one where the appropriate $\beta_0 + \beta_1$ result in the smallest value of $f(\beta_0,\beta_1)$.

Now that β_0 and β_1 are defined for the best fit line, a linear equation can be written as

$$\hat{Y}_i = \beta_0 + (\beta_1 * X_i).$$

Note that $\hat{Y}_i = Y_i + \varepsilon_i$, or the dependent variable for the best fit line equals the dependent variable in the ordered pair plus the residual error.

Now the concept of Error Sum of Squares (SSE) and Total Sum of Squares (SST) is explained. The SSE is defined as the sum of the squares of the difference in the dependent variable from the best fit line and the dependent variable from the ordered pair

$$SSE = \Sigma (\hat{Y}_i - Y_i)^2 \qquad \text{(Devore 1995).}$$

This is how much error is not accounted for in the best fit line, or unexplained error. For a valid regression, the unexplained error, SSE, is minimized. The Total Sum of Squares is a measure of the total variance in the observed Y_i values versus assuming a constant mean average for all the dependent values

$$SST = \Sigma (Y_i - Ybar_i)^2$$

where Ybar is the mean of all the dependent variables in the ordered pairs (Devore 1995). The SST gives the user a gauge to decide the importance of the linear relationship. Small values of SST indicate that a simple mean is sufficient to predict the values of the dependent variable.

Another statistic principle required for this study is the Coefficient of Determination (r^2) (Devore 1995). This statistic is the proportion of the observed error in Y that can be explained by the simple linear regression model.

$$r^2 = 1 - (SSE/SST)$$

Large values of r^2 indicate that the simple linear regression closely models the true regression.

The final concepts are the confidence interval and the prediction interval. The confidence interval is a range of $Y\hat{}_i$ values. For a 95 percent confidence interval, the user can be sure that at least 95 percent of the dependent variables for a certain value of the independent variable will fall within the upper and lower bounds defined by the equations listed below. Likewise, a 95 percent prediction interval tells the user that for a given value of the independent variable, there is a 95 percent chance that a new ordered pair with the same value for the independent variable will have a dependent variable value that falls with in the lower and upper bounds (Devore 1995).

$$CI = xbar \pm \sigma/\sqrt{n}$$

$$PI = xbar \pm \tau_{\alpha/2,\, n-1} * s * \sqrt{(1+1/n)}$$

Here xbar is the mean of the dependent variables along a constant independent variable line. σ is the standard deviation of the population, and n is the number of ordered pairs

with the particular independent variable value of interest. τ indicates a "T" distribution with α being the interval percentage of interest. S represents the sample standard deviation.

These simple principles describe a 2-dimensional linear relationship with only one independent variable. For three indicators, such as relative humidity, ceiling height and station pressure, the linear equation is modified from a 2-dimensional plot to a 4-dimensional plot.

$$\mathbf{Y_i = \beta_0 + (\beta_1 * X_i) + (\beta_2 * Z_i) + (\beta_3 * P_i) + \varepsilon_I}$$ (Devore 1995).

For N number of indicators, the equation is easily modified into an N+1-dimensional equation

$$\mathbf{Y_i = \beta_0 + (\beta_1 * X_i) + (\beta_2 * Z_i) + \ldots + (\beta_N * N_i) + \varepsilon_I}$$ (Devore 1995).

The program "Statistix" mentioned in section 4.1.b, handles up to 30,000 cells of data. In other words, if the regression to be tested has 29 independent variables and one dependant variable, only 1,000 radiation fog events could be investigated to develop the regression line. This restriction did not inhibit the research for each station individually, but taken as a whole to assess applicability for wide spread application a more powerful means of calculating the coefficients was necessary. For this increased power, a matrix form of the linear regression equation was developed in "MATHCAD". A template of this method is shown in Figure 4.5.

$$y := \begin{bmatrix} 4.41 \\ 6.81 \\ 5.26 \\ 5.99 \\ 5.92 \\ 6.14 \\ 6.84 \\ 5.87 \\ 7.03 \\ 6.89 \\ 7.87 \end{bmatrix} \qquad x := \begin{bmatrix} 1 & 44 & 16 & 36 \\ 1 & 15 & 31 & 34 \\ 1 & 48 & 21 & 29 \\ 1 & 21 & 22 & 25 \\ 1 & 8 & 20 & 30 \\ 1 & 81 & 28 & 28 \\ 1 & 45 & 30 & 20 \\ 1 & 84 & 25 & 22 \\ 1 & 64 & 32 & 21 \\ 1 & 25 & 29 & 31 \\ 1 & 23 & 34 & 16 \end{bmatrix}$$

Defines the Dependent and independent variables.

$$\beta_{hat} := \left(x^T \cdot x\right)^{-1} \cdot x^T \cdot y \qquad \beta_{hat} = \begin{bmatrix} 4.13 \\ -0.011 \\ 0.135 \\ -0.035 \end{bmatrix}$$

Calculates the Coefficients.

Figure 4.5. Linear Regression MATHCAD Template. This template calculates the coefficients required for the linear regression.

A more robust template, which not only solves for the coefficients but also calculates the sum of squares error, sum of squares residual, sum of squares total, the confidence interval and the prediction intervals is listed in Appendix A.5.

4.3 Final Data Filtering

Before the data could be put into the regression sequence and the coefficients found, certain filters had to be applied to the data. These filters ensured that the fog reported in the observation was, in fact, radiation fog and not caused by advection, frontal passage, or precipitation-induced cooling.

The filters applied were taken from the Wright-Patterson Radiation Fog Decision Checklist contained in their Local Area Forecast Procedures notebook (WPAFB LAFP

1999). It was assumed that the forecaster applies these decision tools routinely when deciding if radiation fog is probable.

The first filter applied to the data set was timing. As seen in Section 4.1, most fog events did occur in the early morning. Therefore, a timing restriction of four hours was applied around 1200 UTC. Thus, observations before 1000 UTC and after 1400 UTC were deleted.

The next filter was precipitation. Recall that there is a column that accounts for precipitation that occured in the previous 12 hours. Since this is in place, and a stable atmosphere is required for radiation fog, all visibility obscurations that did not include "FG", "BR", "MIFG", or "NONE" were deleted.

Since this study deals with radiation fog, a clear sky plays a major part in the filtering. Observations that had "NONE" in the obscuration column and a ceiling entry below 25,000' were deleted. This ensured that long wave radiation from the earth could exit, thus cooling the surface and potentially developing radiation fog.

Events with missing data were then deleted ensuring that all pertinent information was available for analysis. Finally, since fog events can intensify and then dissipate within the four hours from 1000 UTC to 1400 UTC, each day in the remaining data set was examined and only the minimum visibility was retained. This, in effect, indicates the severity of the fog event. The lower the visibility, the more severe the event. Although a great deal of data was deleted during this filtering, over 4,000 combined fog events remained for the regression.

4.4 Simple Linear Regression of Single Parameters

Recall from section 3.4 that indicators were derived to map the six key factors in fog development: moisture, pressure falls, radiational cooling, condensation nuclei, mixing and a shallow boundary layer. Each of these indicators, or independent variables, was plotted versus visibility for each station. These plots have the ordered pairs, the best fit line, the confidence and the prediction intervals all plotted. The plot and the corresponding r^2 for each indicator for Wright-Patterson are presented in Figures 4.6. through 4.14. Results were similar for Scott and Ft Campbell.

The first indicator examined was moisture. For this factor, two indicators were chosen. First, the number of hours of precipitation that occurred before the fog event is plotted versus the minimum visibility in Figure 4.6. In this case the r^2 value is 0.0882 indicating that less then 9% of the total error can be explained by the linear relationship between visibility in fog and the number of hours precipitation occurred in the last 12 hours. The graph shows that even with no precipitation in the last 12 hours, visibility ranges from unrestricted to totally obscured, but with 12 hours of precipitation, visibility was restricted to less then 3000 meters.

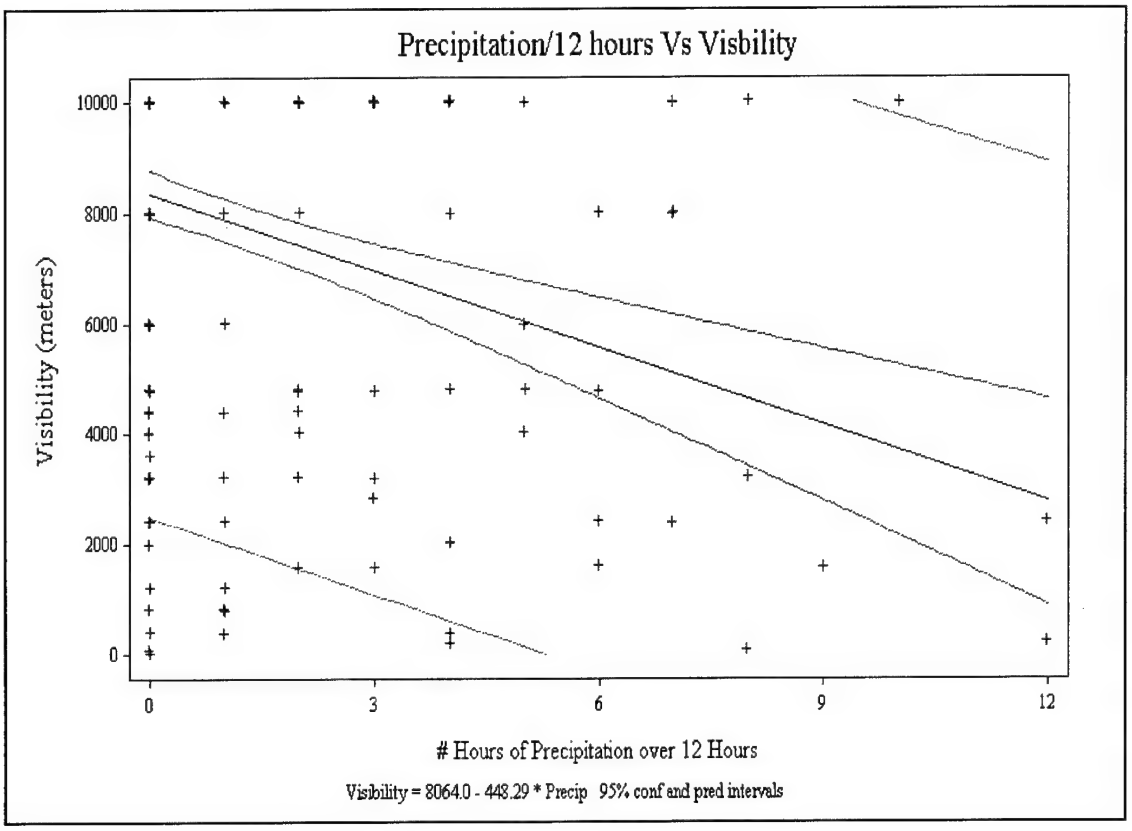

Figure 4.6. Precipitation/12 Hours Vs Visibility. Here the number of hours precipitation occurred in the previous 12 hours is plotted versus the resulting visibility.

The second indicator for moisture was the change in relative humidity over 12 hours. The change in humidity was selected over the forecasted humidity for two key reasons. First, recall from section 2.1.d. that visibility restricting fog can occur in an environment with a relative humidity as low as 75%. In addition, the weather observers are taught that restrictions to visibility that occur with temperature and dew point spreads in excess of 5°C should be attributed to haze, not fog. Therefore, some events that are fog events could be wrongly encoded as haze. The change in relative humidity takes into account moisture advection, cooling, and transpiration. Figure 4.7 points out that for most restrictions to visibility to occur, the change in relative humidity must be positive. No restriction to visibility was recorded for changes in relative humidity of –0.1 or less. The r^2 value for this parameter was 0.13.

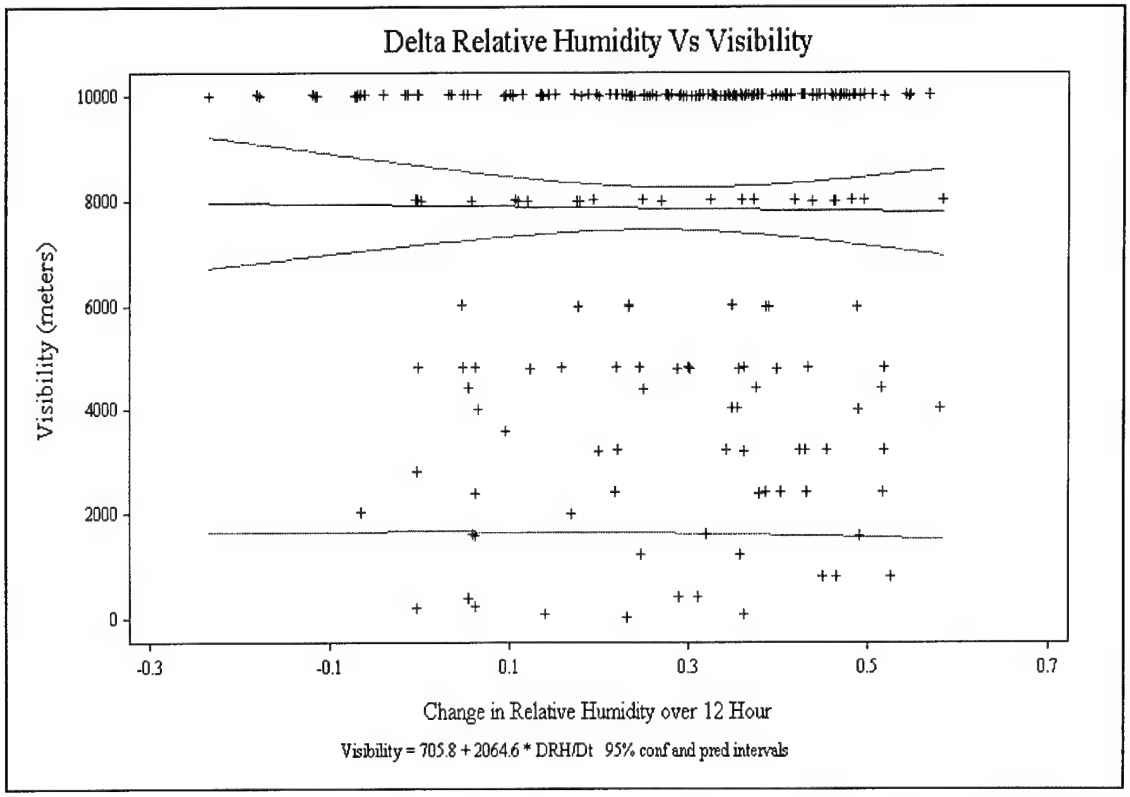

Figure 4.7. Delta Relative Humidity/12 Hours Vs Visibility. The change in RH over the 12 hours before the fog event is plotted versus the resulting visibility.

The next parameter investigated was pressure change. To map this change, the change in pressure over the 12 hours before the fog event occurred was plotted against the corresponding visibility in Figure 4.8. Contrary to the initial assumption, pressure change values for visibility less then 4800 meters (3 statue miles) was slightly skewed toward the positive. Readings ranged from –0.2 to 0.3 inches of mercury per 12 hours. Still, the general trend is toward lower values of visibility with greater drops in pressure. The r^2 value for this parameter was 0.006, indicating that less then one percent of the error can be accounted for by linear regression.

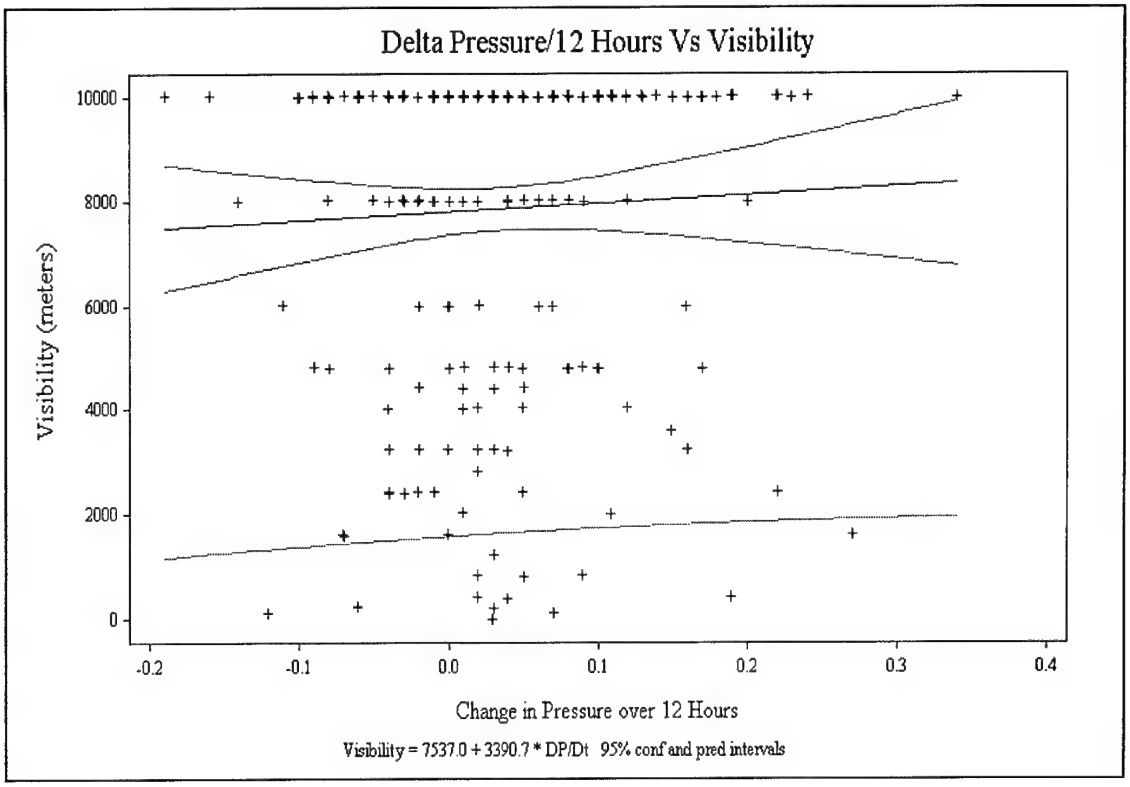

Figure 4.8. Delta Pressure/12 Hours Vs Visibility. The change in surface pressure (inches of mercury per 12 hours) was plotted verses the resulting visibility.

The third key factor scrutinized was radiational cooling of the Earth. For this parameter, three separate indicators were used. First, the amount of clear skies in the last 12 hours was investigated. For this the number of hours in the last 12 hours before the fog event occurred that had ceilings above 25,000 feet were plotted against visibility. Figure 4.9. showed that clear skies was only a moderate factor. The r^2 value for this indicator was 0.077, i.e., less than eight percent of the error is explained by ceiling height.

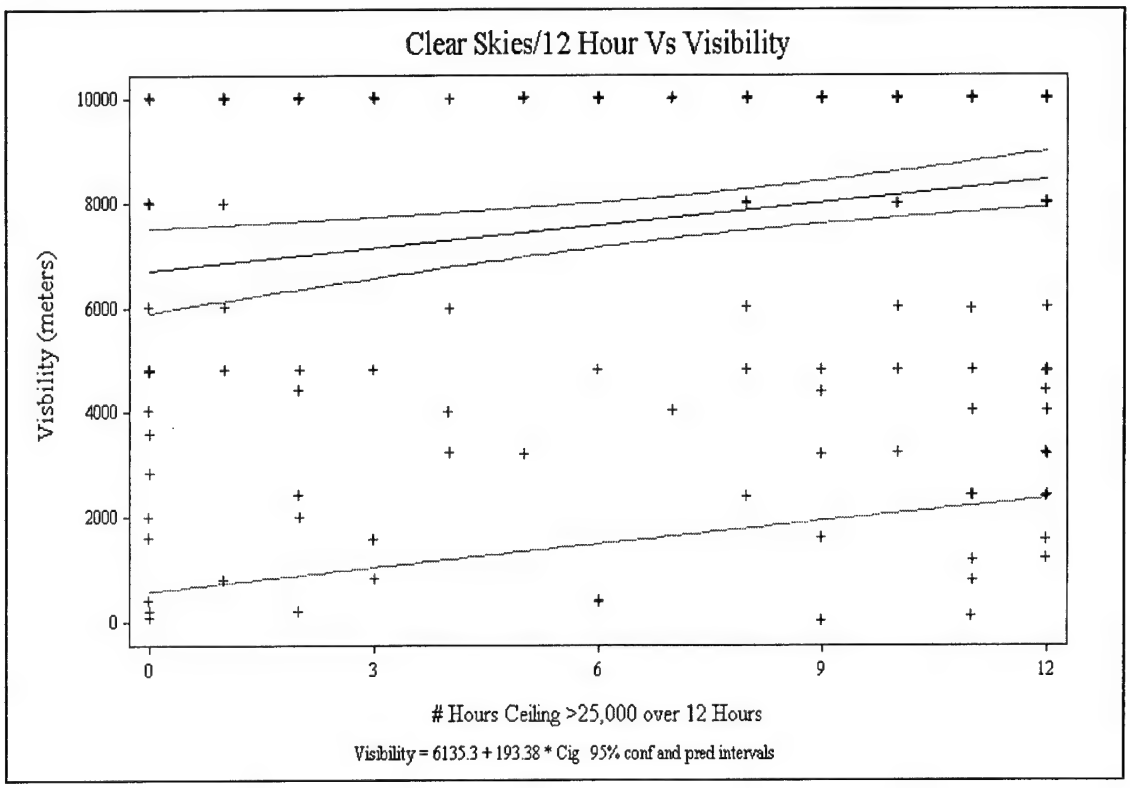

Figure 4.9. Clear Skies/12 Hours Vs Visibility. Here the number of hours the weather station reported ceilings above 25,000' for the previous 12 hours is plotted verses the resulting visibility.

In addition to ceiling height, the change in temperature over 12 hours was analyzed. Figure 4.10. showed falling temperatures did dominate the data. It is interesting, however, that temperature drops greater then 13 °C did not result in significant fog. This is perhaps a result of frontal passage where, although the temperature drops rapidly, drying is occurring and the dew point drops match the temperature drops keeping a constant or slightly decreasing relative humidity. The resulting r^2 value for this indicator was 0.037.

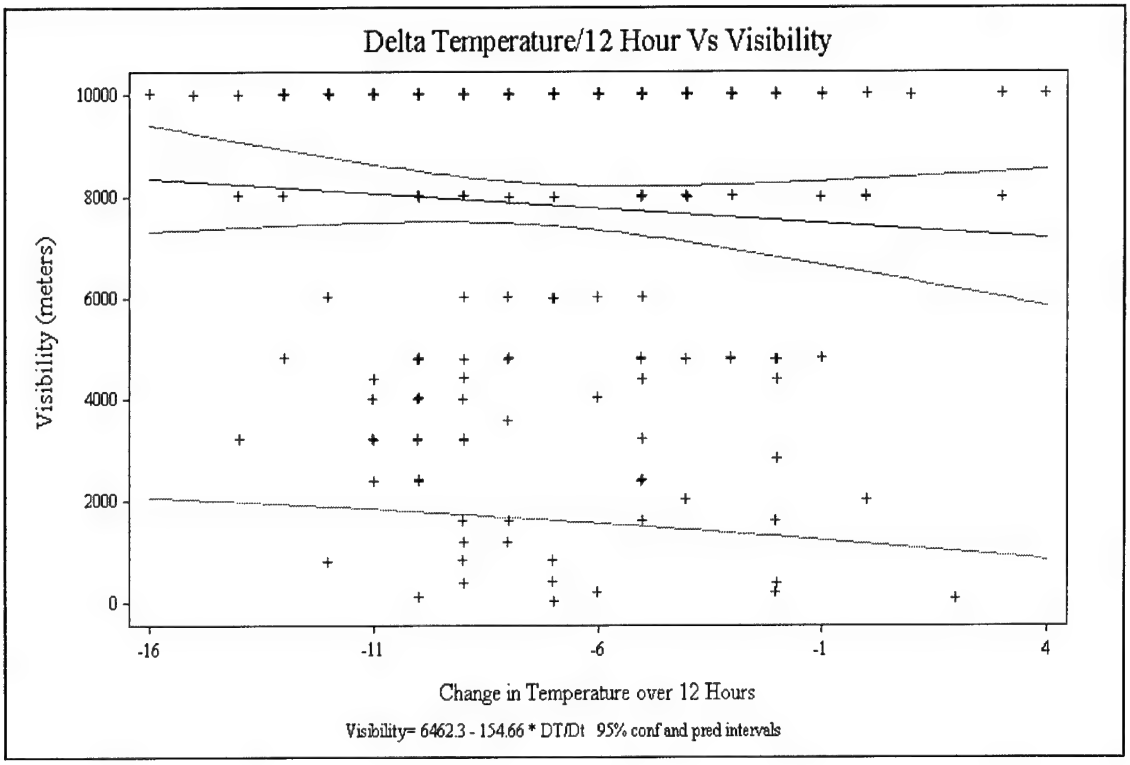

Figure 4.10. Delta Temperature/12 Hours Vs Visibility. Here the change in surface temperature over the previous 12 hours was plotted verses the resulting visibility.

Closely tied to temperature change was the change in dew point over 12 hours. The graph in Figure 4.11. showed a slight negative trend. Values of the change in dew point when fog occurred were between 5.0°C and –7.0°C over 12 hours. This is an important concept for forecasters to keep in mind. Many forecasters use the Air Weather Service rule of thumb that the dew point at maximum heating will be the minimum temperature for the night. However, this graph shows that the dew point regularly drops in the early morning hours, and thus the temperature may fall lower. For this indicator, the r^2 value was 0.002.

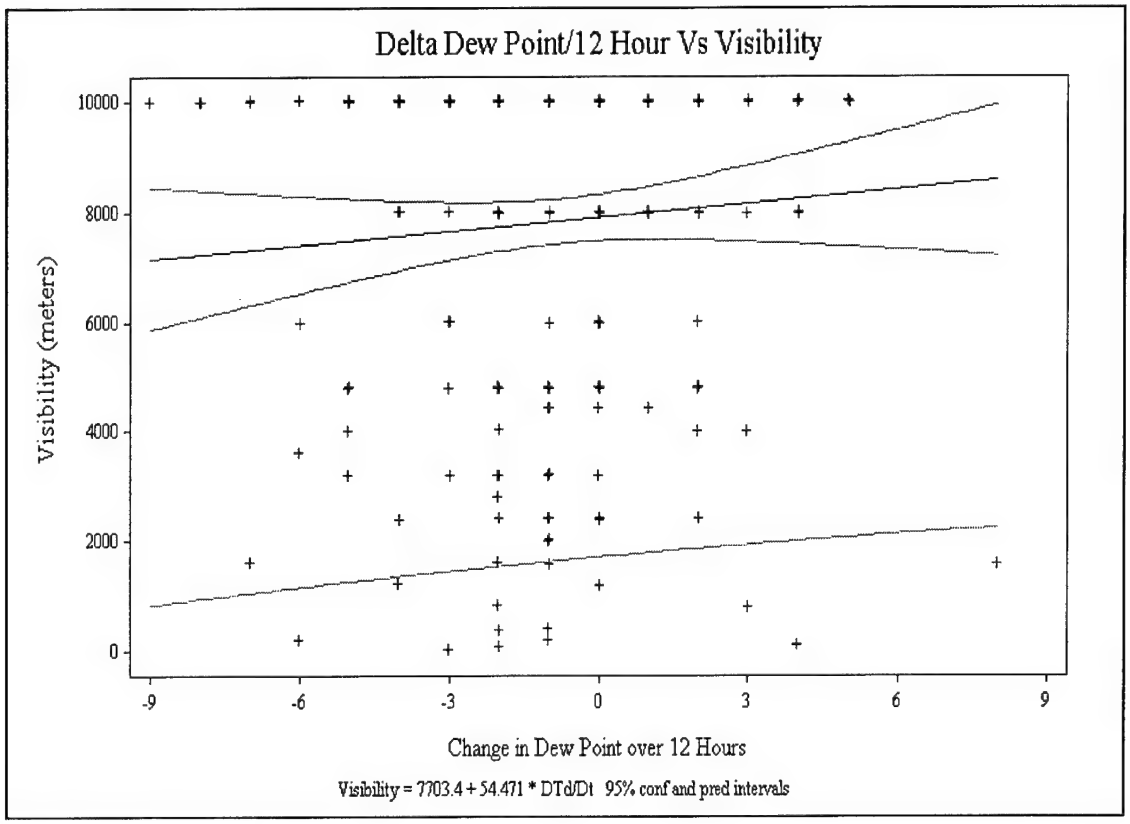

Figure 4.11. Delta Dew Point/12 hours Vs Visibility. Here the change in surface dew point over 12 hours was plotted verses the resulting visibility.

The fourth consideration was condensation nuclei. Again, this indicator was parameterized using the obscuration "HZ". A total amount of hours with haze in the previous 12 hours was plotted versus visibility. The plot in Figure 4.12 shows that the greater the number of haze hours reported, the lower the resulting visibility. However, like the other graphs, visibilities ranged from unrestricted to totally obscured when no haze was reported in the previous 12 hours. The r^2 value for this indicator was 0.051.

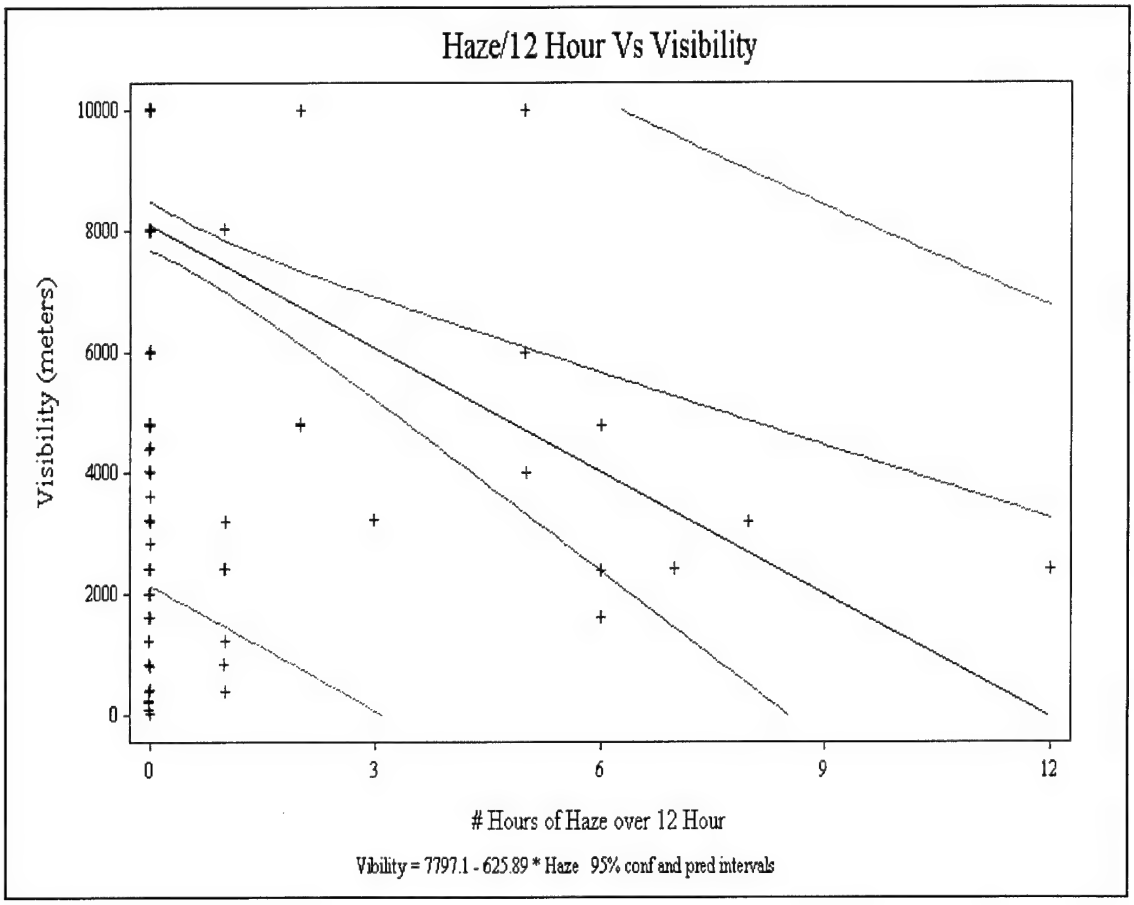

Figure 4.12. Haze/12 Hours Vs Visibility. In this graph the number of hours that the weather station reported haze as an obscuration over the past 12 hours is plotted verses the resulting visbility.

Selecting the wind speed column parameterized mixing. This was a simple plot of the wind speed in knots versus the visibility. Again, Figure 4.13. does not show any significant biases or particular insight into the development of radiation fog. Wind speeds from zero to five knots had corresponding visibilities from unrestricted to totally obscured. The r^2 value for wind speed was 0.008.

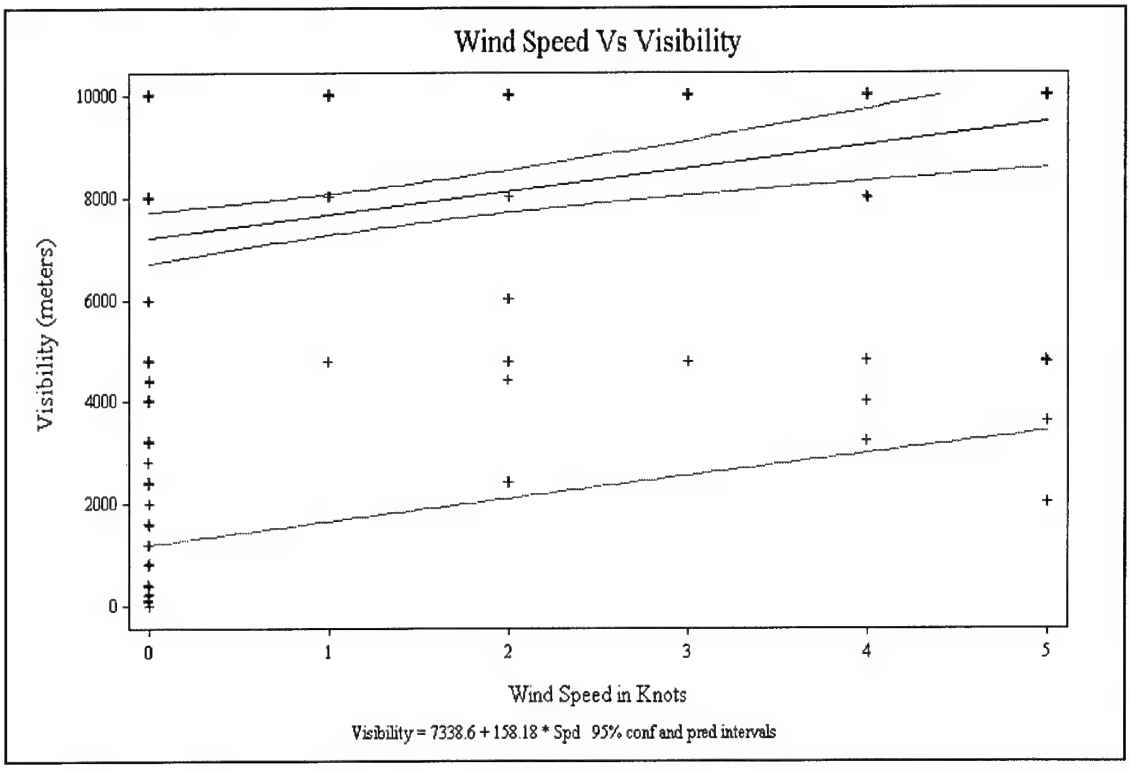

Figure 4.13. Wind Speed Vs Visibility. Wind speed in knots plotted against the resulting visibility.

The final parameter to be investigated was the height of the LCL. The height of the LCL illustrates how much of the atmosphere must be saturated. With a low LCL, the inversion is near the surface and ground moisture can be readily mixed into the air causing saturation and fog. For higher LCLs, more moisture is required to saturate the layer. In addition, more mixing is required to distribute the moisture and more cooling is required for the layer to reach saturation. Here, the height of the LCL in meters is plotted against the visibility. Again, mixed findings are present in the graph. It is apparent from Figure 4.14. that restrictions in visibility due to fog occur when the LCL is at its lowest values. However, values of zero for the LCL resulted in visibility ranging from zero to unrestricted. The r^2 value for this parameter was 0.115.

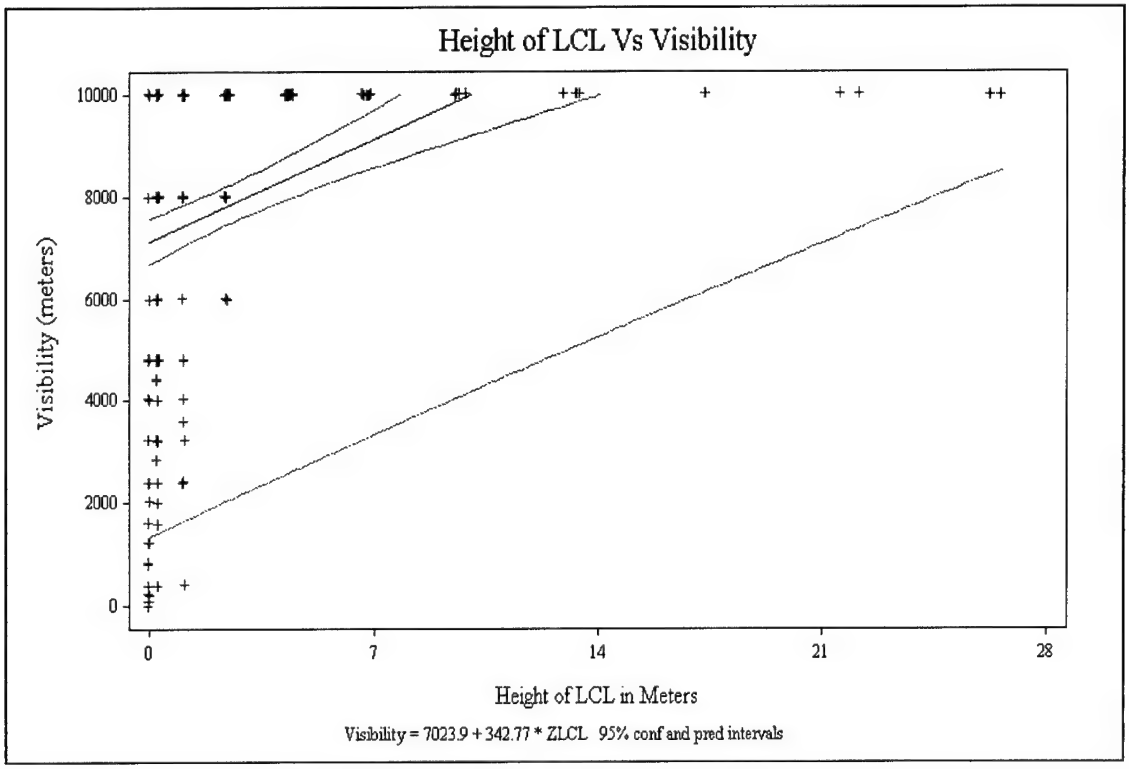

Figure 4.14. Height of LCL Vs Visibility. Here the height of the LCL is plotted against the resulting visibility.

From the previous graphs, it is obvious that no single parameter adequately captures the variability of radiation fog formation. In fact, the graphs show that no linear equation, in any form, exponential, trigonometric, or quadratic closely maps the dependent variables values. Clearly, another method of attack such as multiple regression was required to adequately model radiation fog formation using a linear regression algorithm.

4.5 Multiple Regression of all Parameters

Since single parameters did not perform well as models for fog formation, a combination of parameters must be used. Recall from section 2.1 that fog is formed not from one factor but from a combination of several key factors that come together in a correct mixture. To find the most important ingredients for radiation fog formation, all 23 parameters were imported into the "Statistix" program. Each parameter, its coefficient, and its r^2 value at each location is listed in Tables 4.1 through 4.3.

The two most important results of Tables 4.1 through 4.3 are the following. First, even with 23 different parameters included, the linear regression can only account for just over half the total error. The second and perhaps most interesting finding is that the top four parameters with the highest r^2 values are not only the same in each location but are the same ranking in each location. These top four parameters are, in order of rank, the forecasted ceiling, the forecasted relative humidity, the pressure of the LCL, and the height of the LCL.

Linear regression calculations were made for each separate location and for all three locations together using just the top four parameters. This resulted in four new sets of coefficients. These new equations were then applied to the verification data to check

the ability of the equations to forecast fog. The new equation verification statistics were compared to the Fog Stability Index statistics.

Table 4.1. Parameter Results for Scott AFB. All the parameters investigated for inclusion into the linear regression with the resulting correlation coefficient for Scott AFB.

PARAMETERS FOR SCOTT AFB, IL		
PREDICTOR	COEFFICIENT	INDIVIDUAL R^2
CONSTANT	1.379E+07	N/A
MONTH	47.6722	-0.001
WIND DIRECTION	0.46311	0.010
WIND SPEED	163.666	0.008
FORECASTED TEMPERATURE	-19960.2	0.045
FORECASTED DEW POINT	70056.4	0.084
FORECASTED PRESSURE	3620.12	0.012
FORECASTED CEILING	12.6192	0.341
FORECASTED RELATIVE HUMIDITY	-124517	0.278
850 MB TEMPERATURE	-6.38097	0.048
850 MB DEW POINT	-3.55208	0.068
850 MB WIND DIRECTION	0.34825	0.025
850 MB WIND SPEED	26.9027	0.080
TEMPERATURE OF LCL	-50027.8	0.093
PRESSURE OF LCL	-3746.71	0.241
HEIGHT OF LCL	716.452	0.138
# HOURS CEILING >25,000'	-119.414	0.093
CHANGE IN PRESSURE/12 HOURS	22.1871	0.022
CHANGE IN TEMPERATURE/12 HOURS	-295.367	0.129
CHANGE IN DEW POINT/12 HOURS	232.495	0.002
CHANGE IN RELATIVE HUMIDITY/12 HOURS	-2852.23	0.073
# HOURS OF PRECIPITATION	34.5205	0.113
# HOURS OF HAZE	-363.936	0.051
CEILING 12 HOURS BEFORE	0.62173	0.082
TOTAL R^2 FOR ALL PARAMETERS COMBINED		0.6147

Table 4.2. Parameter Results for Wright-Patterson AFB. All the parameters investigated for inclusion into the linear regression with the resulting correlation coefficient for Wright-Patterson AFB.

PARAMETERS FOR WRIGHT-PATTERSON AFB, OH

PREDICTOR	COEFFICIENT	INDIVIDUAL R^2
CONSTANT	2470703	N/A
MONTH	82.4963	-0.001
WIND DIRECTION	0.52673	0.005
WIND SPEED	78.8174	0.008
FORECASTED TEMPERATURE	724.248	0.053
FORECASTED DEW POINT	8235.16	0.095
FORECASTED PRESSURE	-5969.72	0.029
FORECASTED CEILING	11.7781	0.342
FORECASTED RELATIVE HUMIDITY	-14016.1	0.235
850 MB TEMPERATURE	-7.22172	0.054
850 MB DEW POINT	1.25321	0.068
850 MB WIND DIRECTION	-1.03056	0.0
850 MB WIND SPEED	35.6985	0.024
TEMPERATURE OF LCL	-8992.68	0.104
PRESSURE OF LCL	6059.17	0.183
HEIGHT OF LCL	-217.549	0.115
# HOURS CEILING >25,000'	-27.8412	0.077
CHANGE IN PRESSURE/12 HOURS	-286.841	0.006
CHANGE IN TEMPERATURE/12 HOURS	-269.658	0.037
CHANGE IN DEW POINT/12 HOURS	280.900	0.002
CHANGE IN RELATIVE HUMIDITY/12 HOURS	-4765.38	0.013
# HOURS OF PRECIPITATION	-40.6036	0.087
# HOURS OF HAZE	-321.368	0.051
CEILING 12 HOURS BEFORE	0.61356	0.035
TOTAL R^2 FOR ALL PARAMETERS COMBINED		0.5331

Table 4.3. Parameter Results for Ft Campbell AAF. All the parameters investigated for inclusion into the linear regression with the resulting correlation coefficient for Scott AFB.

PARAMETERS FOR FT CAMPBELL, KY		
PREDICTOR	COEFFICIENT	INDIVIDUAL R^2
CONSTANT	3.352E+07	N/A
MONTH	0.00503	0.0
WIND DIRECTION	-0.12775	0.002
WIND SPEED	162.131	0.005
FORECASTED TEMPERATURE	-58920.2	0.082
FORECASTED DEW POINT	180533	0.132
FORECASTED PRESSURE	33906.3	0.026
FORECASTED CEILING	11.8589	0.289
FORECASTED RELATIVE HUMIDITY	-247088	0.2741
850 MB TEMPERATURE	-5.33446	0.065
850 MB DEW POINT	-2.57601	0.122
850 MB WIND DIRECTION	0.17711	0.0
850 MB WIND SPEED	37.4833	0.019
TEMPERATURE OF LCL	-121542	0.142
PRESSURE OF LCL	-36412.6	0.238
HEIGHT OF LCL	2255.75	0.148
# HOURS CEILING >25,000'	-54.7276	0.119
CHANGE IN PRESSURE/12 HOURS	-846.670	0.015
CHANGE IN TEMPERATURE/12 HOURS	-211.618	0.130
CHANGE IN DEW POINT/12 HOURS	149.484	0.0
CHANGE IN RELATIVE HUMIDITY/12 HOURS	-1572.85	0.050
# HOURS OF PRECIPITATION	-5.55510	0.142
# HOURS OF HAZE	-502.780	0.073
CEILING 12 HOURS BEFORE	0.48740	0.091
TOTAL R^2 FOR ALL PARAMETERS COMBINED		0.5554

4.6 Verification of New Fog Regression Equations and Fog Stability Index

This section takes the four key indicators discovered in section 4.5 and uses the year of data for each location reserved for verification to test the forecast accuracy of the new equations. The new equations are listed below. Each location's verification data has the location-specific equation, the general equation (coefficients derived from all three locations together), and the Fog Stability Index equation applied.

General:

13100+((11.769)*(Forecast Ceiling Height))+((-22410)
***(Forecast Relative Humidity))+((392.139)*(Pressure of the LCL))**
+((-264.172)*(Height of the LCL))

Scott Specific:

31891.8+((12.354)*(Forecast Ceiling Height))+((-19627.5)
***(Forecast relative Humidity))+((-328.527)*(Pressure of the LCL))**
+((-361.522)*(Height of the LCL))

Wright-Patterson Specific:

4768.5+((12.8501)*(Forecast Ceiling Height))+((-21433)
***(Forecast Relative Humidity))+((647.131)*(Pressure of the LCL))**
+((-217.914)*(Height of the LCL))

Ft Campbell Specific:

24950.9+((11.347)*(Forecast Ceiling Height))+((-18833.3)
***(Forecast Relative Humidity))+((-126.654)*(Pressure of the LCL))**
+((-248.998)*(Height of the LCL))

Fog Stability Index:

$$FI = 4*T_s-2*(T_{850}+T_{ds})+W_{850}$$

For these equations the forecasted ceiling height is reported in hundreds of feet, i.e., 100 = 10,000 feet. The forecasted relative humidity is a unitless ration of the vapor pressure to the saturation vapor pressure. The pressure of the LCL is reported in inches of mercury and the height of the LCL is reported in meters. The temperature and dew

point values are all reported in degrees Celsius and the wind speed at 850 mb is reported in knots.

The resultant, a stability index score in the case of the Fog Stability Index, and a forecasted visibility in meters for the specific and general linear regression equations, were used to calculate a positive forecast (fog was forecast) or a negative forecast (no fog forecasted).

In the case of the Fog Stability Index (FSI), a value of less then 31 indicates a high probability that fog will occur as reported in Figure 2.5. For this purpose calculated values of FSI that were less then 31 were considered a positive forecast and values equal to or exceeding 31 were considered to be a negative forecast.

Likewise, visibility forecast values using the specific and general form of the linear regression were calculated. Values less then 8000 meters (5 miles) were considered positive forecasts while values exceeding 8000 meters were considered negative forecasts.

Any data point where the encoded visibility was less then 9999 meters (unrestricted) was considered to be a fog day and visibilities equal to 9999 meters were considered non-fog days.

With this convention in place the total number of fog days were calculated by summing the total number of observations with visibility less than 9999 meters. The total number of positive forecasts were also summed in a like manner. Forecasts for visibility less than 8000 meters or a Stability Index of less then 31 were summed as positive forecasts.

Figures 4.15. through 4.18. are 2X2 contingency tables (probability boxes) for each location. Each probability box has the calculated values for each set of equations: FSI (italics), site specific (underlined), and general (bold). They show the four possibilities for each forecast. The four possibilities are that fog was forecast and did occur (upper left), fog was forecast but did not occur (upper right), fog was not forecast but did occur (lower left) and finally fog was not forecast and did not occur (lower right). These boxes correspond to terms familiar to forecasters looking at forecast statistics: hits (upper left), misses (lower left), false alarms (upper right) and persistence (lower right).

Table 4.4. 2X2 Contengency Table. Here all the possible outcomes for each forecast is illustrated.

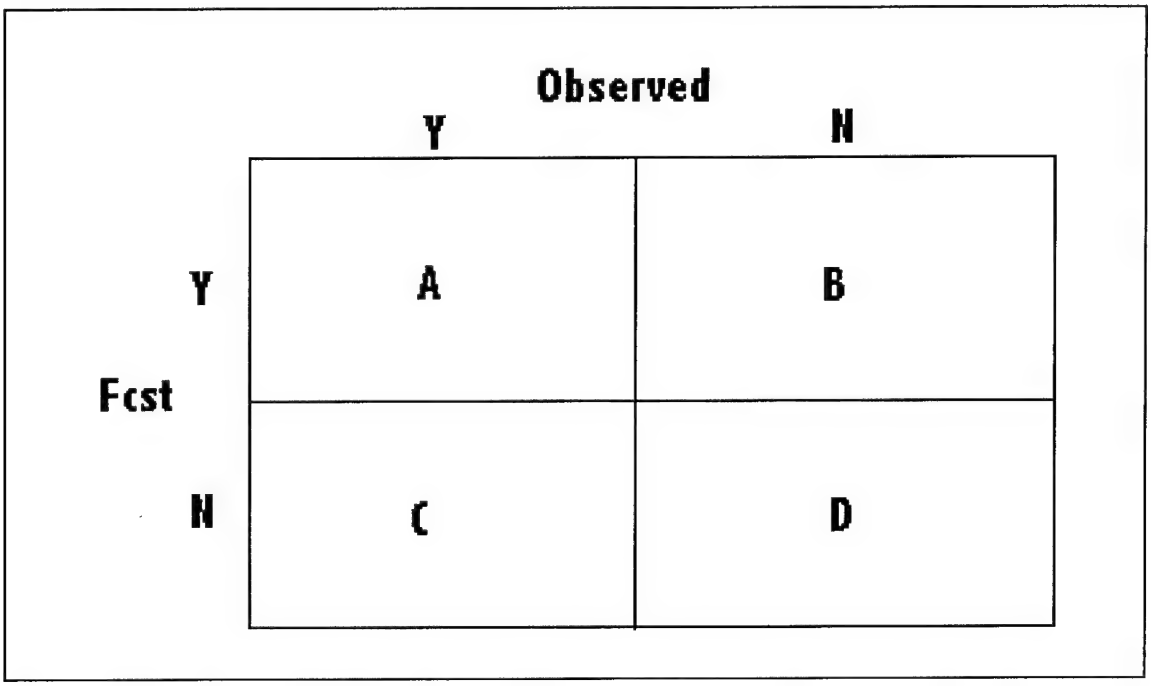

Hit rate is calculated by taking the number of correct forecast and dividing that by the sample size (the sum of all four blocks) **Hit Rate = (A+D)/(A+B+C+D)** (Wilks 1995). In other words, how often was the forecast procedure correct. The false alarm rate is calculated by dividing the number of times fog was forecasted and did not occur

by the total number of times fog was forecasted **False Alarm = (B)/(A+B)** (Wilks 1995). Perhaps more important is the Threat Score. This score takes the number of correct positive forecast and divides it by the total sum minus the correct negative forecast **Threat Score = (A)/(A+B+C)** (Wilks 1995).

Table 4.5. Probability Box for Scott AFB. Recorded are the number of each forecast type that either correctly or incorrectly predicted fog formation. FSI is in italics, the site specific equation is underlined and the general equation output is in bold.

Verification Square for Scott AFB, IL

FSI, Specific Equation, **General Equation**
Total Cases=307

	Fog Occured	Fog Did Not Occur
Fcst Yes	*11* 143 **143**	*14* 57 **57**
Fcst No	*128* 14 **14**	*154* 93 **93**

Table 4.6. Probability Box for Wright-Patterson AFB. Recorded are the number of each forecast type that either correctly or incorrectly predicted fog formation. FSI is in italics, the site specific equation is underlined and the general equation output is in bold.

Verification Square for Wright-Patterson AFB, OH

FSI, Specific Equation, **General Equation**
Total Cases = 118

	Fog Occured	Fog Did Not Occur
Fcst Yes	*4* 46 **46**	*9* 33 **39**
Fcst No	*33* 3 **3**	*72* 36 **30**

Table 4.7. Probability Box for Ft. Campbell AAF. Recorded are the number of each forecast type that either correctly or incorrectly predicted fog formation. FSI is in italics, the site specific equation is underlined and the general equation output is in bold.

Verification Square for Ft Campbell, KY

FSI, Specific Equation, **General Equation**
Total Cases = 151

	Fog Occured	Fog Did Not Occur
Fcst Yes	*5* 40 **29**	*6* 6 **4**
Fcst No	*60* 31 **42**	*80* 74 **76**

Table 4.7. Verification Results. The Hit Rate, False Alarm Rate and the Threat Score for each regression and the Fog Stability Index for each location.

Verification Rates			
	Fog Stability Index	Site Specific	General Equation
Scott			
Hit Rate	54%	77%	77%
False Alarm Rate	56%	29%	29%
Threat Score	7%	67%	67%
Wright-Pat			
Hit Rate	64%	69%	64%
False Alarm Rate	69%	42%	46%
Threat Score	9%	56%	52%
Ft Campbell			
Hit Rate	56%	75%	70%
False Alarm	55%	13%	12%
Threat Score	7%	52%	39%

4.7 Summary of Findings and Conclusions

As illustrated in Table 4.7, both the general and the site-specific linear regression equations outperform the Fog Stability Index.

When applied to Scott, the general linear equation gave the exact same forecast as the site-specific equation for each case. The regression models outperformed the Fog Stability Index in hit rate by 23 percentage points. The false alarm rates were also cut by 27 percent when the linear regression model was used. The major improvement was in threat score. The new equations scored 60 percentage points better then the Fog Stability Index.

Wright-Patterson had slightly different results. Although the general equation scored the same hit rate as the Fog Stability Index, the site-specific equation scored five

points higher. False Alarm rates were better by 23 to 27 percentage points. In addition, the threat score differed by over 40 percentage points. Still, Wright-Patterson's scores were closer then either other station. This could be a result of the low number of fog events in the verification data set.

Ft Campbell's scores were very similar to the results seen for Scott AFB. In general the hit rate improved by 15 to 20 percentage points by using the new regression formulas. The false alarm rates decreased by over 40 points. But, again, the real improvement could be seen in the threat score. Even the general regression equation out performed the Fog Stability Index by 32 percentage points.

In general, the linear regression models slightly improve the fog forecast over using the Fog Stability Index when hit rate alone is investigated. The real differences are evident in the false alarm rates. Improvements in this arena range from 23 to 43 percent. However, the real payoff is in the threat score. Improvements over the Fog Stability Index range from 32 to 60 percentage points. This is a significant improvement, which outweighs the added investment in time needed to calculate the pressure and the height of the LCL.

5. Recommendations for Future Work

5.1 Improvements in Regression Analysis

If additional work is to be accomplished using this data set, there are four concerns that should be addressed. First, frontal passage effects were considered nullified by the removal of strong winds. Second, the surface parameters should be expanded to include entries not routinely encoded in the observations. Next, additional upper air data is available and should be considered as a possible parameter. Finally, different regression techniques should be investigated.

To eliminate frontal passage effects on the data the change in wind direction should be investigated. Wind shifts of over 30 degrees with sustained winds of 10-15 knots could indicate strong frontal passage. In this case, the entire day should be deleted from the data set. Additionally, rapidly falling dew points could indicate a change in air mass, frontal passage.

In addition to frontal features, hydro-meteorological parameters should be expanded. Instead of looking at the number of hours rain fell in the previous 12 hours, rain fall rates or intensities may play a larger role. Ground moisture, if parameterized correctly, coupled with ground temperature could be the key to accurately forecasting radiation fog. A method of measuring or predicting the size of condensation nuclei at the airfield could focus the study from when visibility will be reduced to when sufficient condensation will form on the nuclei.

Not only are surface features critical, but this research has shown that upper air features play an important role as well. Consider using the 925 mb level instead of, or in addition to, the 850 mb level. Non-mandatory levels could provide a wealth of data not

routinely utilized. In addition, Doppler radar provides rapidly updated profiles of the environmental wind fields.

Finally, one could examine other regression techniques besides linear regression. Logistic regression with a yes or no forecast for fog could be more accurate.

5.2 Improvements in Verification Analysis

Suggestions to improve the scope and impact of this study would include expanding the number of fog indexes investigated, working to improve or tailor existing fog indexes, or developing an index for the timing or severity of radiation fog events.

There are a great many fog indexes. They are listed in the Air Force Weather Agency's Met-Tips. These indexes use surface, upper-air, climotology and a host of other sources to make forecast. Additional work could focus more on improving existing forecast techniques. Fine tuning a technique grounded in principle and being familiar to counter forecasters may lead to a significant improvement in fog forecasting skill. Finally, this thesis dealt with simply forecasting whether radiation fog was likely to occur between 1000 UTC and 1400 UTC. A study of the severity or the time of onset could greatly improve the fog forecasting skill of Air Force Weather Forecasters.

BIBLIOGRAPHY

Ahrens, C. Donald. Meteorology Today. St. Paul: West Publishing Company, 1988. pp.126, 171-175, 562.

Air Force Combat Climotology Center. "AFCCC." Excerpt from the Operational Climatic Data Summary, n. pag. **http://www.afccc.af.mil**. 12 December 1999.

Air Force Weather Agency (AFWA). Meteorological Techniques. Technical Note 98/002. Offutt Air Force Base, Nebraska: HQ AFWA, 15 July 1998.

Air Weather Service (AWS). T-TWOS: The Fog Stability Index. T-TWOS #29. Hurlburt Field, Florida: Detachment 4, HQ AWS Technology Applications, 1990.

Bohren, C. F. Clouds in a Glass of Beer. New York: John Wiley & Sons, Inc., 1987. pp 1.

Croft P. J., Pfost R. L., Medlin J. M., Johnson G. A., Fog Forecasting in the Southern Region: A Conceptual Model Approach, *Weather and Forecasting*, 12, 1997.

Devore, J. L. Probability and Statistics for Engineering and the Sciences 4th Edition. Pacific Grove: Brooks/Cole Publishing Company, 1995 pp 278, 296, 477-489.

Duffield G. F. and Nastrom, G. D. Equations and Algorithms for Meteorological Applications in Air Weather Service. Air Weather Service Technical Regulation 83-001. Scott Air Force Base, Illinois: HQ AWS 30 December 1983.

Fleagle, R. G. and Businger, J. A. An Introduction to Atmospheric Physics 2nd Edition. San Diego: Academic Press, Inc., 1980. pp 72, 297, 298.

Ft Campbell Army Air Field. "Terminal Forecast Reference Notebook (TFRN)." Forecast guide for local forecasters, 19th ASOS, Ft Campbell AAF, Kentucky. August 1999.

Griend, A.A. van de and Camillo, P. J., "Estimation of Soil Moisture from Diurnal Surface Temperature Observations," Proceedings of IGARSS' 86 Symposium. 1227-1230. Zurich: ESA Publications Division, August 1986.

Holton, J. R. An Introduction to Dynamic Meteorology, 3rd Edition. San Diego: Academic Press, Inc., 1992. pp 19.

Iribarne, J. V. and Cho, H. R. Atmospheric Physics. Boston: D. Reidel Publishing Company, 1980. pp 65, 87.

Lala, G.G. "Radiation Fog: Characteristics and Formation Processes," AIAA 25th Aerospace Sciences Meeting. New York: American Institute of Aeronautics and Astronautics, January 12-15, 1987.

Ritchie, Randal R. Technical Sergeant, USAF, Senior Counter Forecaster, Wright-Patterson Air Force Base, Ohio. Personal interview 1996.

Rogers, R. R. and Yau, M. K. A Short Course in Cloud Physics Third Edition. Woburn: Butterworth-Heinemann, 1989. pp 16.

Schanda, E. Physical Fundamentals of Remote Sensing. New York: Springer-Verlag, 1986. pp 106.

Scott Air Force Base. "Terminal Forecast Reference Notebook (TFRN)." Forecast guide for local forecasters, 375th Operations Support Squadron, Scott AFB, Illinois. December 1999.

Wallace, J. M. and Hobbs, P. V. Atmospheric Science. San Diego: Academic Press, Inc., 1977. pp 77, 216, 228.

Wilks D. S., Statistical Methods in the Atmospheric Sciences. San Diego: Academic Press, Inc.,1995. pp 240-241.

Wright-Patterson Air Force Base (WPAFB). "Local Analysis and Forecast Program (LAFP)." Forecast guide for local forecasters, 88th Weather Squadron, Wright-Patterson AFB, Ohio. June 1999.

Wright-Patterson Air Force Base (WPAFB). "Terminal Forecast Reference Notebook (TFRN)." Forecast guide for local forecasters, 88th Weather Squadron, Wright-Patterson AFB, Ohio. June 1999.

Appendix

A.1. Surface Data Interpretation Program

```
pro temp

;*********************************************************************
;       This program reads in the data from a formatted surface observations file
;       and saves the data into a 21 X n array.  Each element in that row has a
;       specific (i,j) position.
;
;       Written By: Capt Jim Trigg
;       Last Modified: 12 Dec 99
;       Files Required: Surface data in a 22 column format with a '&' separating
;                       the columns.
;*********************************************************************
; closes all devices left open

        close,/all

;allows selection of a specific file

        fn=dialog_pickfile(filter="~/")

;if no file is selected the program is exited

        if (fn eq "") then return

;just a counter to determine the total number of sfc ob files that will be read

        openr,2,fn
        n=0L

; defines a string variable

        s=""

;  returns the number of rows in the file

        while not (EOF(2)) do begin
                readf,2,s
                n=n+1
        endwhile

        total=n-1
```

```
        close,2
;read file elements into an array

        openr,2,fn
        readf,2,s

;reads in each row as a single string variable to determine the number of columns

        lines=strarr(total)
        readf,2,lines
        close,2
        data = strarr(22,total)
print, 'read the lines'

;*****************************************************************
;uses a loop to separate out each element in each row to a specific array value by using
;the '&' symbol as the identifier(this identifier is what is used in ;each sfc ob file)
;*****************************************************************

        for i=0l,total-1 do data(*,i)=str_sep(lines(i),"&")

; This identifies the variable associated with each column of the array

wmo = data[0,*]
ymd = data[1,*]
year = data[2,*]
month = data[3,*]
day = data[4,*]
type = data[5,*]
time = data[6,*]
DSG = data[7,*]
dir = data[8,*]
spd = data[9,*]
gust = data[10,*]
vis = data[11,*]
wx = data[12,*]
skycon = data[13,*]
temp = data[14,*]
dp = data[15,*]
press = data[16,*]
cig = data[17,*]
rmks = data[18,*]
satvappress = data[19,*]
vappress = data[20,*]
rh = data[21,*]
```

```
;changes the values of temp and Dp from string variables to numbers

temp=fix(temp)
dp=fix(dp)

print, 'seperated the data'

;This identifies where the missing values of temp are

blanks = Where(strpos(temp, '99') GE 0, bc)
nonblank = Where(strpos(temp, '99') LT 0, nbc)

;find obs before 99 with number

for i = 0L, bc-1 do begin
        before = max(where(nonblank LT blanks(i)))
        after = min(where(nonblank GT blanks(i)))

;Calculates the missing value

        temp(blanks(i)) = temp(nonblank(before)) + ((temp(nonblank(after))-$
        temp(nonblank(before))) * (float(blanks(i) - $
        nonblank(before))/float(nonblank(after) -  nonblank(before))))
endfor

;This identifies where the missing values of DP are

blank = Where(strpos(dp, '99') GE 0, bc)
nonblanks = Where(strpos(dp, '99') LT 0, nbc)

print, 'identified the blanks'

;Find obs before 99 with number

for i = 0L, bc-1 do begin

        before = max(where(nonblanks LT blank(i)))
        after = min(where(nonblanks GT blank(i)))

;calculates the missing values

        dp(blank(i)) = dp(nonblanks(before)) + ((dp(nonblanks(after))- $
        dp(nonblanks(before))) * (float(blank(i) -$
        nonblanks(before))/float(nonblanks(after)-nonblanks(before)) ) )
endfor
```

```
print, 'calculated the blanks'

; changes the values of temp and DP into strings and removes the spaces

temp=strcompress(string(temp))
dp=strcompress(string(dp))

; formats the output

output=strarr(total)
output=(wmo+'&'+ymd+'&'+year+'&'+month+'&'+day+'&'+type+'&'+time+'&'+dsg+ $
        '&' +dir+'&'+spd+'&'+gust+'&'+vis+'&'+wx+'&'+skycon+'&'+temp+'&'+dp+'&' $
       +press+'&'+cig+'&'+rmks+'&'+satvappress+'&'+vappress+'&'+rh)

print, 'recompiled the data'

;Opens the output file

openu, outfile, "hop98.txt", /get_lun

;prints the output to the file

printf, outfile, output

;closes the file

close, outfile
free_lun, outfile

print, 'wrote the file'

end
```

Appendix A.2. Upper-Air Data Interpretation Program

```
pro uainterp

;*****************************************************************
;       This program will read in ua data and interpret the  missing values
;
;       Written By: Capt Jim Trigg
;       Last Modified: 12 Dec 99
;       Files Required: UA data in a 11 column format with a '&' separating the columns
;*****************************************************************

; closes all devices left open

        close,/all

;allows selection of a specific file

        fn=dialog_pickfile(filter="~/")

;if no file is selected the program is exited

        if (fn eq "") then return

;just a counter to determine the total number of lines in the file

        openr,2,fn
        n=0L

; defines a string variable

        s=""

;  returns the number of rows in the file

        while not (EOF(2)) do begin
                readf,2,s
                n=n+1
        endwhile

        total=n-1

        close,2
```

```
;reads file elements into an array and reads in each row as a single string variable to
;determine the number of columns

        openr,2,fn
        lines=strarr(total)
        readf,2,lines
        close,2
        data = strarr(11,total)
print, 'read the lines'

;*************************************************************************
;       uses a loop to separate out each element in each row to a specific array value by
;       using the '&' symbol as the identifier(this identifier is what is used in each
;       ua file)
;*************************************************************************

        for i=0l,total-1 do data(4:10,i)=str_sep(lines(i),"&")

print, 'sorted the data'

; This identifies the variable associated with each column of the array

code = data[4,*]
press = data[5,*]
hgt = data[6,*]
temp = data[7,*]
dp = data[8,*]
dir = data[9,*]
spd = data[10,*]

;converts the string temperature and dew point string variables into numbers

tmp=fix(data(7,*))
dp=fix(data(8,*))

print, 'seperated the data'

; This identifies where the missing values of temp are (32767)

blanks = Where(tmp EQ 32767, bc)
nonblank = Where(tmp NE 32767, nbc)
```

```
; find obs before and after 32767

for i = 0L, bc-1 do begin
        before = max(where(nonblank lt blanks(i)))
        after = min(where(nonblank GT blanks(i)))

;Calculates the missing value

        tmp(blanks(i)) = tmp(nonblank(before)) + ( (tmp(nonblank(after))- $
        tmp(nonblank(before)))* ( float(blanks(i) -$
        nonblank(before))/float(nonblank(after)-nonblank(before)) ) )
endfor

print, 'calculated the temps'

; This identifies where the missing values of dewpoint are (32767)

        blanks = Where(dp EQ 32767, bc)
        nonblank = Where(dp NE 32767, nbc)

; find obs before and after 32767

for i = 0L, bc-1 do begin
        before = max(where(nonblank lt blanks(i)))
        after = min(where(nonblank GT blanks(i)))

;Calculates the missing value

        dp(blanks(i)) = dp(nonblank(before)) + ( (dp(nonblank(after))-$
        dp(nonblank(before)))* ( float(blanks(i) - $
        nonblank(before))/float(nonblank(after)-nonblank(before)) ) )
endfor

print, 'calculated the dps'

;formats the output file

output=strarr(bc)

;converts the temperature and dew point values into strings and removes the spaces
        data(7,*)=strcompress(string(tmp))
        data(8,*)=strcompress(string(dp))
```

```
;formats the output file

        output=(data(0,*)+'&'+data(1,*)+'&'+data(2,*)+'&'+data(3,*)+'&'+data(4,*)+$
        '&'+data(5,*)+'&'+data(6,*)+'&'+data(7,*)+'&'+data(8,*)+'&'+data(9,*)+'&' $
        +data(10,*))

print, 'recompiled the data'

;identifies the location and name for the new file and saves it

file_name='/home/kramer1/users/jtrigg/day9312.txt'
openw,2,file_name
printf,2,output

print, 'wrote the file'

end
```

Appendix A.3. Upper-Air Data Truncation Program

```
pro uatrunc

;*****************************************************************
;       This program will read in ua data and remove the data above 700mb it
;       appends the date and time to each line of the data
;
;       Written By: Capt Jim Trigg
;       Last Modified: 12 Dec 99
;       Files Required: UA data in a 11 column format with a '&' separating the columns
;*****************************************************************

; closes all devices left open

        close,/all

;allows selection of a specific file

        fn=dialog_pickfile(filter="~/")

;if no file is selected the program is exited

        if (fn eq "") then return

;just a counter to determine the total number of lines in the file

        openr,2,fn
        n=0L

; defines a string variable

        s=""

;  returns the number of rows in the file

        while not (EOF(2)) do begin
                readf,2,s
                n=n+1
        endwhile

        total=n-1

        close,2
```

```
;reads file elements into an array and reads in each row as a single string variable to
;determine the number of columns

        openr,2,fn
        lines=strarr(total)
        readf,2,lines
        close,2
        data = strarr(11,total)
print, 'read the lines'

;*********************************************************************
;       uses a loop to separate out each element in each row to a specific array value by
;       using the '&' symbol as the identifier(this indentifier is what is used in each
;       sfc ob file)
;*********************************************************************

        for i=0l,total-1 do data(4:10,i)=str_sep(lines(i),"&")

print, 'sorted the data'

; This identifies the variable associated with each column of the array

code = data[4,*]
press = data[5,*]
hgt = data[6,*]
temp = data[7,*]
dp = data[8,*]
dir = data[9,*]
spd = data[10,*]

;defines the data variable

date=strarr(4,total)
```

```
;calculates the date

for i=0l,total-1 do begin
        if (data(4,i) eq 254) then begin
                date(0,i)=data(5,i)
                date(1,i)=data(6,i)
                date(2,i)=data(7,i)
                date(3,i)=data(8,i)
        endif else begin
                 date(*,i)=date(*,i-1)
                 data(0:3,I)=date(*,i)
        endelse
endfor

;identifies and keeps all the data below 700mb

        keep=where (data(5,*) ge 700, bc)
        data=data(*,keep)

;reformats the data for the new truncated file

        output=(data(0,*)+'&'+data(1,*)+'&'+data(2,*)+'&'+data(3,*)+'&'+data(4,*)+'&'$
              +data(5,*)+'&'+data(6,*)+'&'+data(7,*)+'&'+data(8,*)+'&'+data(9,*)+'&'+$
              data(10,*))

print, 'recompiled the data'

;identifies where the file will be saved and saves the file

file_name='/home/kramer1/users/jtrigg/day9312.txt'
openw,2,file_name
printf,2,output

print, 'wrote the file'

end
```

Appendix A.4. Surface and Upper-Air Compilation Program

```
pro uasfcinter

;*************************************************************************
;       This program will append the 850mb temp, dewpoint and winds to the surface
;       observation
;
;       Written By: Capt Jim Trigg
;       Last Modified: 12 Dec 99
;       Files Required: Surface data in a 22 column format and UA data in a 11 column
;       format each with a '&' separating the columns,
;*************************************************************************

; closes all devices left open

        close,/all

;allows selection of the surface file to be appended to

        fn=dialog_pickfile(filter="")

;if no file is selected the program is exited

        if (fn eq "") then return

;just a counter to determine the total number of sfc ob lines that will be read

        openr,2,fn
        n=0L

;defines a string variable

        s=""

;returns the number of rows in the file

        while not (EOF(2)) do begin
                readf,2,s
                n=n+1
        endwhile

        totals=n
```

```
        close,2

;reads file elements into an array and reads in each row as a single string variable to
;determine the number of columns

        openr,2,fn
        lines=strarr(totals)
        readf,2,lines
        close,2
        datas = strarr(26,totals)

print, 'read the scf lines'

;*****************************************************************
;       uses a loop to separate out each element in each row to a specific array value by
;       using the '&' symbol as the identifier(this identifier is what is used in each
;       sfc ob file)
;*****************************************************************

        for i=0l,totals-1 do datas(0:25,i)=str_sep(lines(i),"&")

print, 'sorted the sfc data'

;*********************************************************************

;allows selection of the ua file to be appended to the sfc file

        fn=dialog_pickfile(filter="")

;if no file is selected the program is exited

        if (fn eq "") then return

;just a counter to determine the total number of UA lines that will be read

        openr,2,fn
        n=0L

; defines a string variable

        s=""

;  returns the number of rows in the file

        while not (EOF(2)) do begin
                readf,2,s
```

```
            n=n+1
        endwhile

        totalu=n
        close,2

;reads file elements into an array and reads in each row as a single string variable to
;determine the number of columns

        openr,2,fn
        lines=strarr(totalu)
        readf,2,lines
        close,2
        datau = strarr(11,totalu)

print, 'read the ua lines'

;*************************************************************
;       uses a loop to separate out each element in each row to a specific array value by
;       using the '&' symbol as the identifier(this identifier is what is used in each
;       UA ob file)
;*************************************************************

        for i=0l,totalu-1 do datau(*,i)=str_sep(lines(i),"&")

print, 'sorted the ua data'

;puts the year code in the UA sounding from a 4 digit number into a two digit number
;to match the sfc data

datau(3,*)=datau(3,*)-1900

;separates out the 850mb data

        keep=where(datau(5,*) eq 850)
        newdatau=fix(datau(*,keep))

;formats the new combined output file

        ntotal=n_elements(newdatau)
```

```
;makes all variables into numbers

datas(2,*)=fix(datas(2,*))
datas(3,*)=fix(datas(3,*))
datas(4,*)=fix(datas(4,*))
datas(6,*)=fix(datas(6,*))
newdatau(0,*)=fix(newdatau(0,*))
newdatau(1,*)=fix(newdatau(1,*))
newdatau(2,*)=fix(newdatau(2,*))
newdatau(3,*)=fix(newdatau(3,*))

;appends the UA data to the new sfc file

q=0
for i=0L,(ntotal/11)-1 do begin

        for j=0l,totals-1 do begin

                if ((newdatau(3,i) eq datas(2,j)) $
                        and (newdatau(2,i) eq datas(3,j)) $
                        and (newdatau(1,i) eq datas(4,j)) $
                        and (((newdatau(0,i) eq 0) and (datas(6,j) le 1159))$
                         or ((newdatau(0,i) eq 12) and (datas(6,j) ge 1200)))) then begin
                datas(22,j)=newdatau(7,i)
                datas(23,j)=newdatau(8,i)
                datas(24,j)=newdatau(9,i)
                datas(25,j)=newdatau(10,i)
                endif else begin q=q+1
                endelse
        endfor
endfor

print, 'appended the data'

;final format of the output file

output=lonarr(totals)

        output=(datas(0,*)+'&'+datas(1,*)+'&'+datas(2,*)+'&'+datas(3,*)+'&'+datas(4,*)$
        +'&'+datas(5,*)+'&'+datas(6,*)+'&'+datas(7,*)+'&'+datas(8,*)+'&'+datas(9,*)+$
        '&'+datas(10,*)+'&'+datas(11,*)+'&'+datas(12,*)+'&'+datas(13,*)+'&'+$
        datas(14,*)+'&'+datas(15,*)+'&'+datas(16,*)+'&'+datas(17,*)+'&'+datas(18,*)+$
        '&'+datas(19,*)+'&'+datas(20,*)+'&'+datas(21,*)+'&'+datas(22,*)+'&'+$
        datas(23,*)+'&'+datas(24,*)+'&'+datas(25,*))
```

```
print, 'recompiled the data'

;identifies the file and location for the appended data then saves it

file_name='/home/kramer1/users/jtrigg/totday93.txt'

openw,2,file_name
printf,2,output

print, 'wrote the file'

end
```

Appendix A.5. Expanded Linear Regression MATCAD Template

ORIGIN≡1

$$y := \begin{bmatrix} 4.41 \\ 6.81 \\ 5.26 \\ 5.99 \\ 5.92 \\ 6.14 \\ 6.84 \\ 5.87 \\ 7.03 \\ 6.89 \\ 7.87 \end{bmatrix} \qquad x := \begin{bmatrix} 1 & 44 & 16 & 36 \\ 1 & 15 & 31 & 34 \\ 1 & 48 & 21 & 29 \\ 1 & 21 & 22 & 25 \\ 1 & 8 & 20 & 30 \\ 1 & 81 & 28 & 28 \\ 1 & 45 & 30 & 20 \\ 1 & 84 & 25 & 22 \\ 1 & 64 & 32 & 21 \\ 1 & 25 & 29 & 31 \\ 1 & 23 & 34 & 16 \end{bmatrix}$$

Check for singularity:

$\left| x^T \cdot x \right| = 6.053 \cdot 10^9$

$n := \text{rows}(y)$

$p := 4$

$ybar := \text{mean}(y)$

$df_{sst} := n - 1 \qquad df_{ssr} := p - 1 \qquad df_{sse} := n - p$

$$\beta_{hat} := \left(x^T \cdot x\right)^{-1} \cdot x^T \cdot y \qquad \beta_{hat} = \begin{bmatrix} 4.13 \\ -0.011 \\ 0.135 \\ -0.035 \end{bmatrix} \qquad y_{hat} := x \cdot \beta_{hat} \qquad e := y - y_{hat} \qquad SSE := e^T \cdot e$$

$SST := (y - ybar)^T \cdot (y - ybar) \qquad SSR := SST - SSE$

$$MSR := \frac{SSR}{df_{ssr}} \qquad MSE := \frac{SSE}{df_{sse}} \qquad F_{star} := \frac{MSR_1}{MSE} \qquad Prob := 1 - pF\left(F_{star_1}, df_{ssr}, df_{sse}\right)$$

ANOVA Table:

Source:	SS	df	MS	F&Prob
Regression	$SSR = (8.798)$	$df_{ssr} = 3$	$MSR = (2.933)$	$F_{star} = (103.995)$
Error	$SSE = (0.197)$	$df_{sse} = 7$	$MSE = (0.028)$	$Prob = 3.614 \cdot 10^{-6}$
	$SST = (8.996)$	$df_{sst} = 10$		

$$Var_{betahat} := MSE_1 \cdot \left(x^T \cdot x\right)^{-1} \qquad s_{\beta 0} := \sqrt{Var_{betahat_{1,1}}} \qquad s_{\beta 1} := \sqrt{Var_{betahat_{2,2}}}$$

$$Var_{yhat} := MSE_1 \cdot \left[x \cdot \left(x^T \cdot x\right)^{-1} \cdot x^T\right]$$

Confidence Intervals

$\alpha := .05$

$\beta_{hat_1} - \left| qt\left(\frac{\alpha}{2}, n-p\right) \right| \cdot s_{\beta 0} = 2.843$

$\beta_{hat_2} - \left| qt\left(\frac{\alpha}{2}, n-p\right) \right| \cdot s_{\beta 1} = -0.016$

$\beta_{hat_1} = 4.13$

$\beta_{hat_2} = -0.011$

$\beta_{hat_1} + \left| qt\left(\frac{\alpha}{2}, n-p\right) \right| \cdot s_{\beta 0} = 5.418$

$\beta_{hat_2} + \left| qt\left(\frac{\alpha}{2}, n-p\right) \right| \cdot s_{\beta 1} = -6.18510^{-3}$

$observation := 6$

$\left(x^T\right)^{\langle observation \rangle}$

$y_{hat_{observation}} - \left| qt\left(\frac{\alpha}{2}, n-p\right) \right| \cdot \sqrt{Var_{yhat_{observation,observation}}} = 5.775$

$y_{hat_{observation}} = 6.03$

$y_{hat_{observation}} + \left| qt\left(\frac{\alpha}{2}, n-p\right) \right| \cdot \sqrt{Var_{yhat_{observation,observation}}} = 6.285$

Prediction Interval

$y_{hat_{observation}} - \left| qt\left(\frac{\alpha}{2}, n-p\right) \right| \cdot \sqrt{MSE_1 + Var_{yhat_{observation,observation}}} = 5.558$

$y_{hat_{observation}} = 6.03$

$y_{hat_{observation}} + \left| qt\left(\frac{\alpha}{2}, n-p\right) \right| \cdot \sqrt{MSE_1 + Var_{yhat_{observation,observation}}} = 6.502$

Vita

Jimmie Lee Trigg, Jr., son of Jim and Freda Trigg, was born on April 5, 1968, in Beckley, West Virginia. He graduated from Embry-Riddle Aeronautical University, Daytona Beach, Florida, in 1990 with a Bachelor of Science degree in Aeronautical Engineering. He then married his college sweetheart, the former Michelle Mallios, daughter of George and Mitzi Mallios of Chicago, Illinois. After graduation, he was commissioned a 2nd Lieutenant in the United States Air Force through the Air Force Reserve Officer Training Program at that university.

Upon commissioning, Jim was selected to attend the University of Oklahoma to study meteorology in the Basic Meteorology Program (BMP). His first assignment after BMP was as a Base Weather Station Operational Counter Forecaster. Later he advanced into the Wing Weather Officer position supporting the 33rd Fighter Wing. He received the Air Force Material Command's "Weather Officer of the Year" award for his support in Dhahran, Saudi Arabia during Operation Southern Watch.

His next assignment was as Flight Commander of the weather flight at Kunsan Air Base, Republic of Korea. After his Korea tour, he was assigned as the Flight Commander of 88th Weather Flight, Wright-Patterson AFB, Ohio. There he distinguished himself through superior support to the base and was awarded his second Air Force Material Command "Weather Officer of the Year" award.

In 1998 he received a regular commission and began his Meteorology program at AFIT. He graduated from AFIT on March 21, 2000 and was then assigned to the 15th Operational Weather Squadron at Scott AFB, Illinois as the commander of the training flight.